Pacific Northwest
NATIONAL LABORATORY

A comparative study of dark matter flow & hydrodynamic turbulence and its applications

May 2022

Zhijie (Jay) Xu
Multiscale Modeling Team
Computational Mathematics Group
Physical & Computational Science Directorate
Zhijie.xu@pnnl.gov; zhijiexu@hotmail.com

U.S. DEPARTMENT OF ENERGY BATTELLE

Preface

Dark matter, if exists, accounts for five times as much as ordinary baryonic matter. Therefore, dark matter flow might possess the widest presence in our universe. The other form of flow, hydrodynamic turbulence in air and water, is without doubt the most familiar flow in our daily life. During the pandemic, we have found time to think about and put together a systematic comparison for the connections and differences between two types of flow, both of which are typical non-equilibrium systems.

The goal of this presentation is to leverage this comparison for a better understanding of the nature of dark matter and its flow behavior on all scales. Science should be open. All comments are welcome.

Thank you!

Data repository and relevant publications

Structural (halo-based) approach:

0.	**Data https://dx.doi.org/10.5281/zenodo.6541230**
1.	Inverse mass cascade in dark matter flow and effects on halo mass functions https://doi.org/10.48550/arXiv.2109.09985
2.	Inverse mass cascade in dark matter flow and effects on halo deformation, energy, size, and density profiles https://doi.org/10.48550/arXiv.2109.12244
3.	Inverse energy cascade in self-gravitating collisionless dark matter flow and effects of halo shape https://doi.org/10.48550/arXiv.2110.13885
4.	The mean flow, velocity dispersion, energy transfer and evolution of rotating and growing dark matter halos https://doi.org/10.48550/arXiv.2201.12665
5.	Two-body collapse model for gravitational collapse of dark matter and generalized stable clustering hypothesis for pairwise velocity https://doi.org/10.48550/arXiv.2110.05784
6.	Evolution of energy, momentum, and spin parameter in dark matter flow and integral constants of motion https://doi.org/10.48550/arXiv.2202.04054
7.	The maximum entropy distributions of velocity, speed, and energy from statistical mechanics of dark matter flow https://doi.org/10.48550/arXiv.2110.03126
8.	Halo mass functions from maximum entropy distributions in collisionless dark matter flow https://doi.org/10.48550/arXiv.2110.09676

Statistics (correlation-based) approach:

0.	**Data https://dx.doi.org/10.5281/zenodo.6569898**
1.	The statistical theory of dark matter flow for velocity, density, and potential fields https://doi.org/10.48550/arXiv.2202.00910
2.	The statistical theory of dark matter flow and high order kinematic and dynamic relations for velocity and density correlations https://doi.org/10.48550/arXiv.2202.02991
3.	The scale and redshift variation of density and velocity distributions in dark matter flow and two-thirds law for pairwise velocity https://doi.org/10.48550/arXiv.2202.06515
4.	Dark matter particle mass and properties from two-thirds law and energy cascade in dark matter flow https://doi.org/10.48550/arXiv.2202.07240
5.	The origin of MOND acceleration and deep-MOND from acceleration fluctuation and energy cascade in dark matter flow https://doi.org/10.48550/arXiv.2203.05606
6.	The baryonic-to-halo mass relation from mass and energy cascade in dark matter flow https://doi.org/10.48550/arXiv.2203.06899

Statistical (correlation-based) approach for dark matter flow

Scale and redshift dependence of density and velocity distributions in dark matter flow

Xu Z., 2022, arXiv:2202.06515 [astro-ph.CO]
https://doi.org/10.48550/arXiv.2202.06515

Introduction

Review:
Statistical theory in hydrodynamic turbulence

- Velocity fluctuation and distributions
- Incompressible on all scales
  - Divergence-free
  - Constant density

- N-body simulations are invaluable tools for DMF:
  - Velocity fluctuation and distributions
  - Density is non-uniform (density fluctuation/distributions)

- Fundamental problems when projecting N-body density/velocity field onto structured grid:
  - N-body fields are sampled discrete locations of particles.
  - The sampling has a poor quality at locations with low particle density

Goal 1: Density distributions and two-point statistics

Goal 2: Velocity distributions and redshift and scale dependence

Halo-based non-projection approach:

- Instead of projecting, analysis is performed by the statistics over all pairs on different scales to maximumly preserve the information from N-body simulation

- Based on the halo description, divide all particles into halos and out-of-halo particles, whose distributions evolve differently

- Scale and redshift dependence of distributions can be studied by the variation of generalized kurtosis for a given distribution.

One-point probability distributions of density field

- Projecting particle field onto structured grid involves information loss and numerical noise.
- Without projecting onto grid, Delaunay tessellation is used to reconstruct the density field and maximumly preserve information in N-body data.
- Compute the volume V_p occupied by every particle

$$\rho(\mathbf{x}) = m_p / V_p$$

Particle density

$$\delta(\mathbf{x}) = \frac{\rho(\mathbf{x})}{\rho_0} - 1$$

Particle density contrast

$$\eta(\mathbf{x}) = \log(1+\delta(\mathbf{x})) = \log\left(\frac{\rho(\mathbf{x})}{\rho_0}\right)$$

Particle log-density

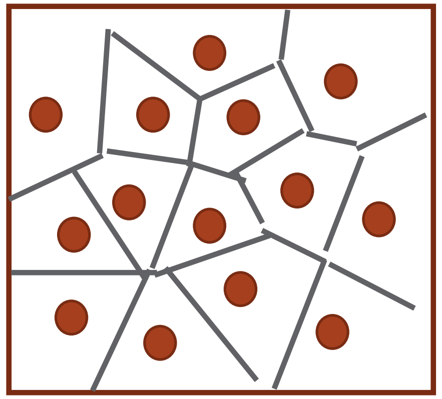

Delaunay tessellation

$$\left\langle \frac{1}{1+\delta(\mathbf{x})} \right\rangle = 1 \qquad \left\langle e^{-\eta(\mathbf{x})} \right\rangle = 1$$

Constraints for density contrast and log-density

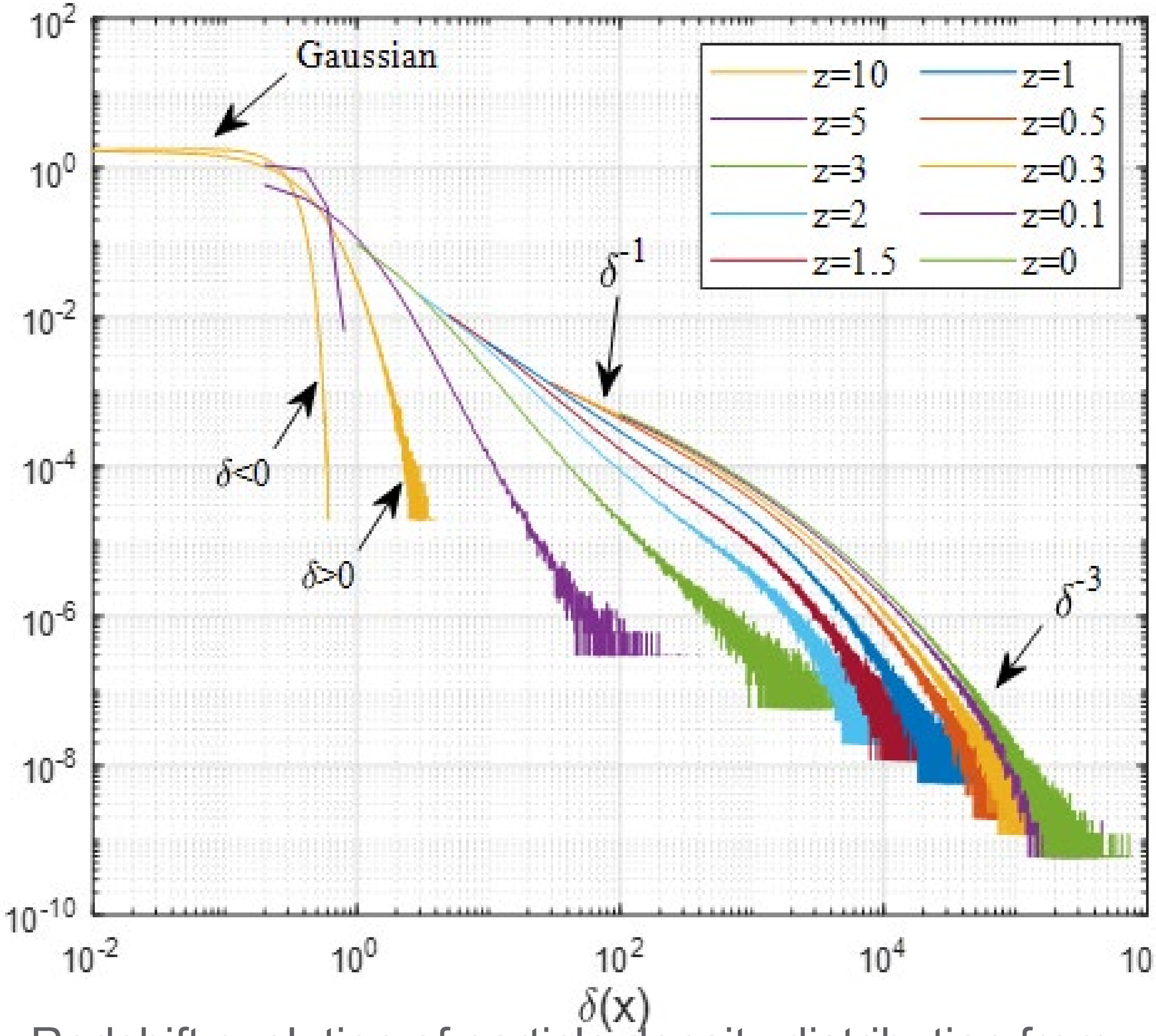

Redshift evolution of particle density distribution from z=10 to z=0. Density evolves from initial Gaussian to an asymmetric distribution with a long tail $\sim\delta^{-3}$

Probability distributions of log-density field

- Gaussian distribution of log-density at high redshift.
- Bimodal distribution of log-density at low redshift.
- Two peaks corresponds to contributions from particles in all halos and particles out-of-halo.
- Best fitted bimodal distribution at z=0 showing fraction of particles in halos is about 60%, consistent with inverse mass cascade theory.

$$f(\eta)=\frac{c_1}{\sqrt{2\pi}\sigma_1}\exp\left[\frac{(\eta-\mu_1)^2}{2\sigma_1^2}\right]+\frac{1-c_1}{\sqrt{2\pi}\sigma_2}\exp\left[\frac{(\eta-\mu_2)^2}{2\sigma_2^2}\right]$$

$$c_1=0.404 \qquad c_2=1-c_1=0.596$$

$$\mu_1=-0.30 \qquad \mu_2=4.256$$

$$\sigma_1=1.212 \qquad \sigma_2=2.979$$

Particles in halos should have an average density close to Δ_c, the critical density ratio $18\pi^2$, such that the mean density for all halo particles $\langle\mu_2\rangle=\log(18\pi^2)\approx 5$

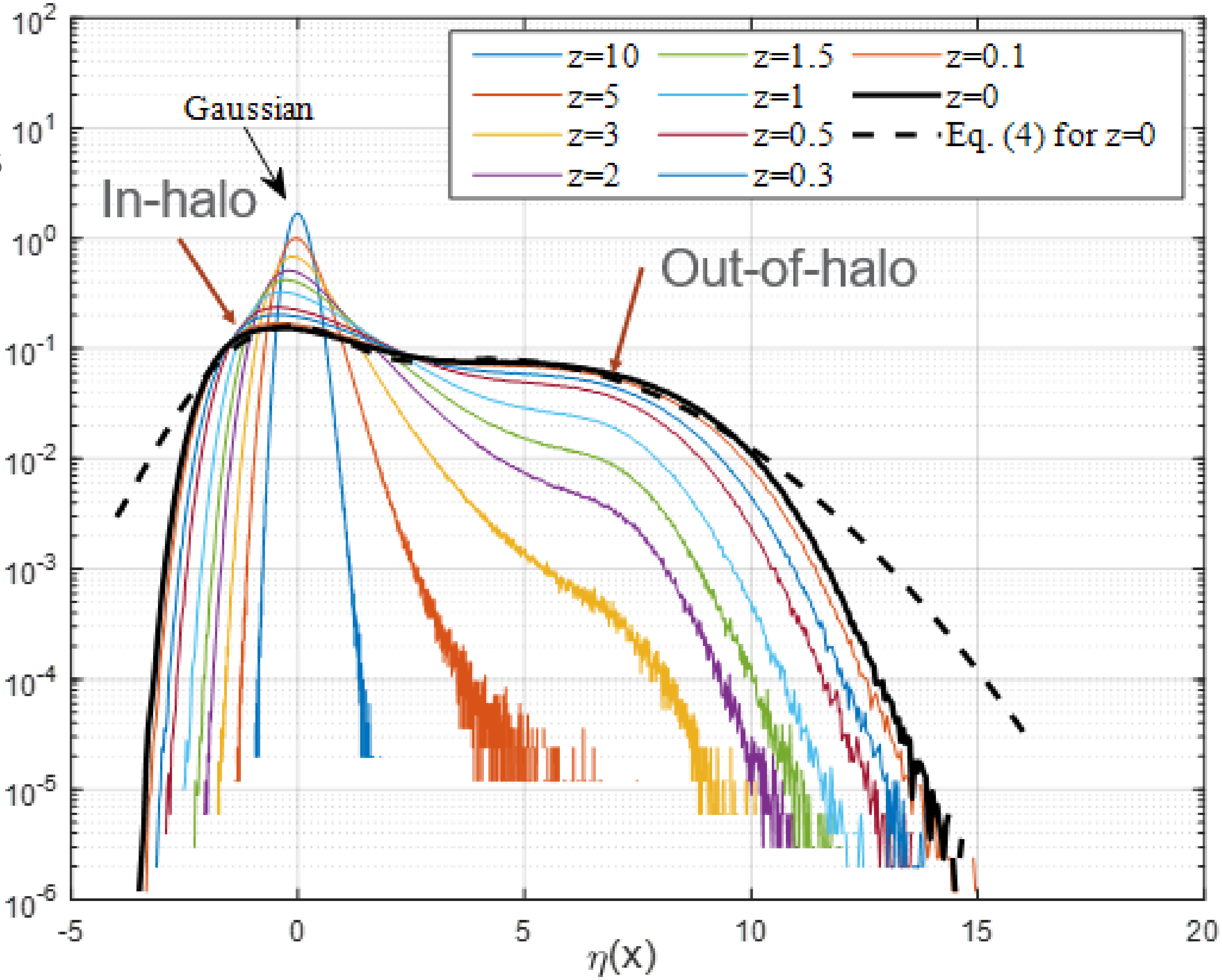

Distribution of log-density at different redshifts z. The log-density evolves from Gaussian to an approximately bimodal distribution at z=0 with two peaks.

Halo-based non-projection approach for particle density

- Checking the density distributions of particles in halos and out-of-halo particles separately.
- Identifying all halos in entire system and dividing all particles into halo and out-of-halo particles.
- For out-of-halo particles, the distribution is relatives Gaussian (or δ is lognormal) with mean density decreasing with time.
- For halo particles, log-density distribution evolves with increasing mean density due to the formation of halos.

Characterizing the time evolution of the shape of distribution by introducing nth order generalized kurtosis:

$$K_n(\tau) = \frac{\left\langle \left(\tau - \langle\tau\rangle\right)^n \right\rangle}{\left\langle \left(\tau - \langle\tau\rangle\right)^2 \right\rangle^{n/2}} = \frac{S_n^{cp}(\tau)}{S_2^{cp}(\tau)^{n/2}}$$ Generalized kurtosis

$$S_n^{cp}(\tau) = \left\langle \left(\tau - \langle\tau\rangle\right)^n \right\rangle$$ nth central moment

For Gaussian: $K_2 = 1 \quad K_4 = 3 \quad K_6 = 15 \quad K_8 = 105 \quad K_3 = K_5 = 0$

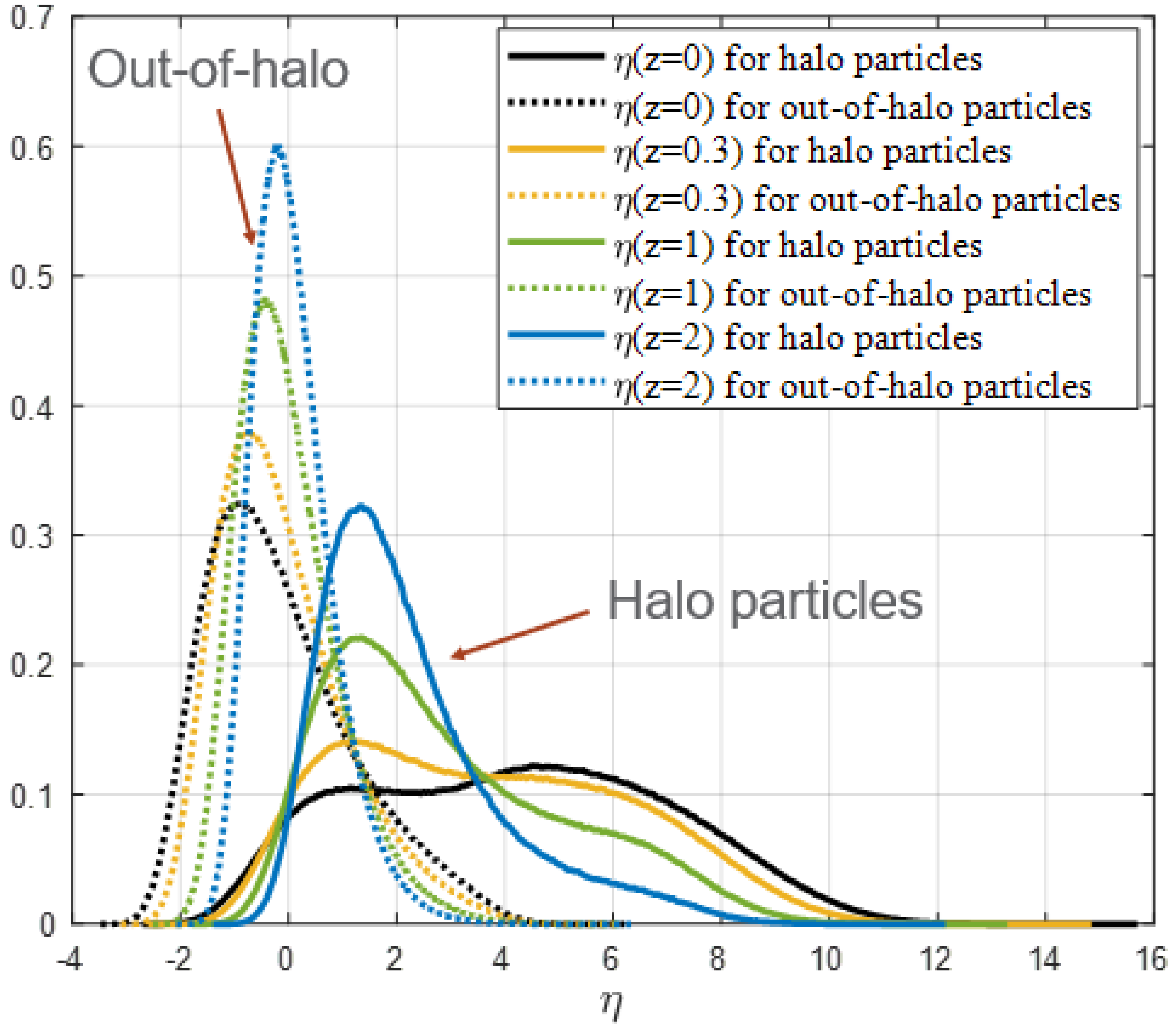

Redshift evolution of log-density distributions for two different types of particles.

Time evolution of comoving particle density field

- Distribution of η is always Gaussian for out-of-halo particles.
- Distribution of δ for out-of-halo particles is approximately log-normal
- Distribution of η for halo particles approaching some symmetric non-Gaussian distribution with vanishing odd order kurtosis

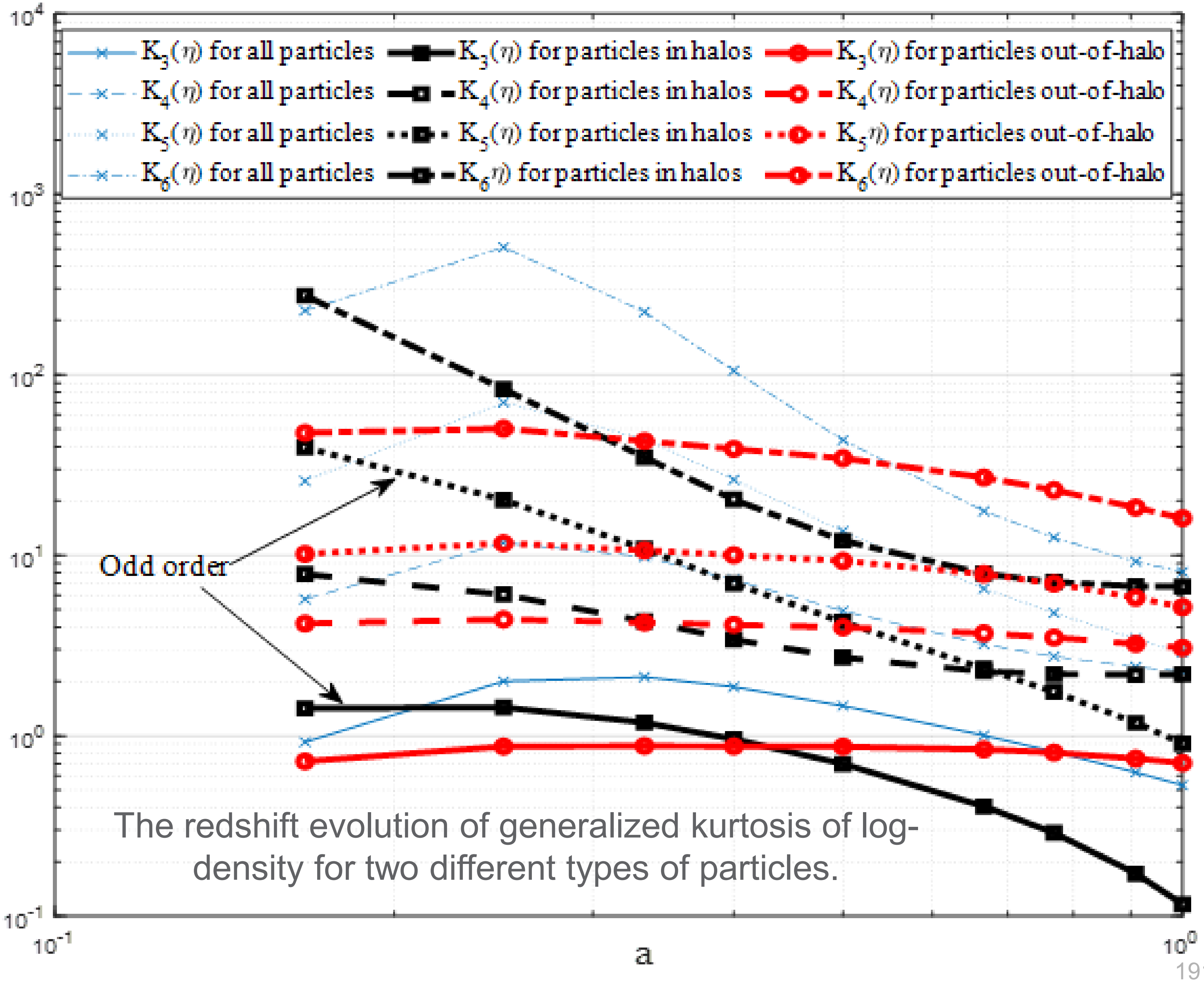

The redshift evolution of generalized kurtosis of log-density for two different types of particles.

Time evolution of particle density field

- For out-of-halo particles, the mean log-density decreases with time and <η><0 after z=1. This reflects less and less out-of-halo particles due to inverse mass cascade.
- For halo particles, mean log-density increasing with time (<η> ~ $a^{1/2}$) reflects more and more particles residing in halos
- For halo particles, standard deviation of log-density increasing with time (std(η) ~ $a^{1/2}$)

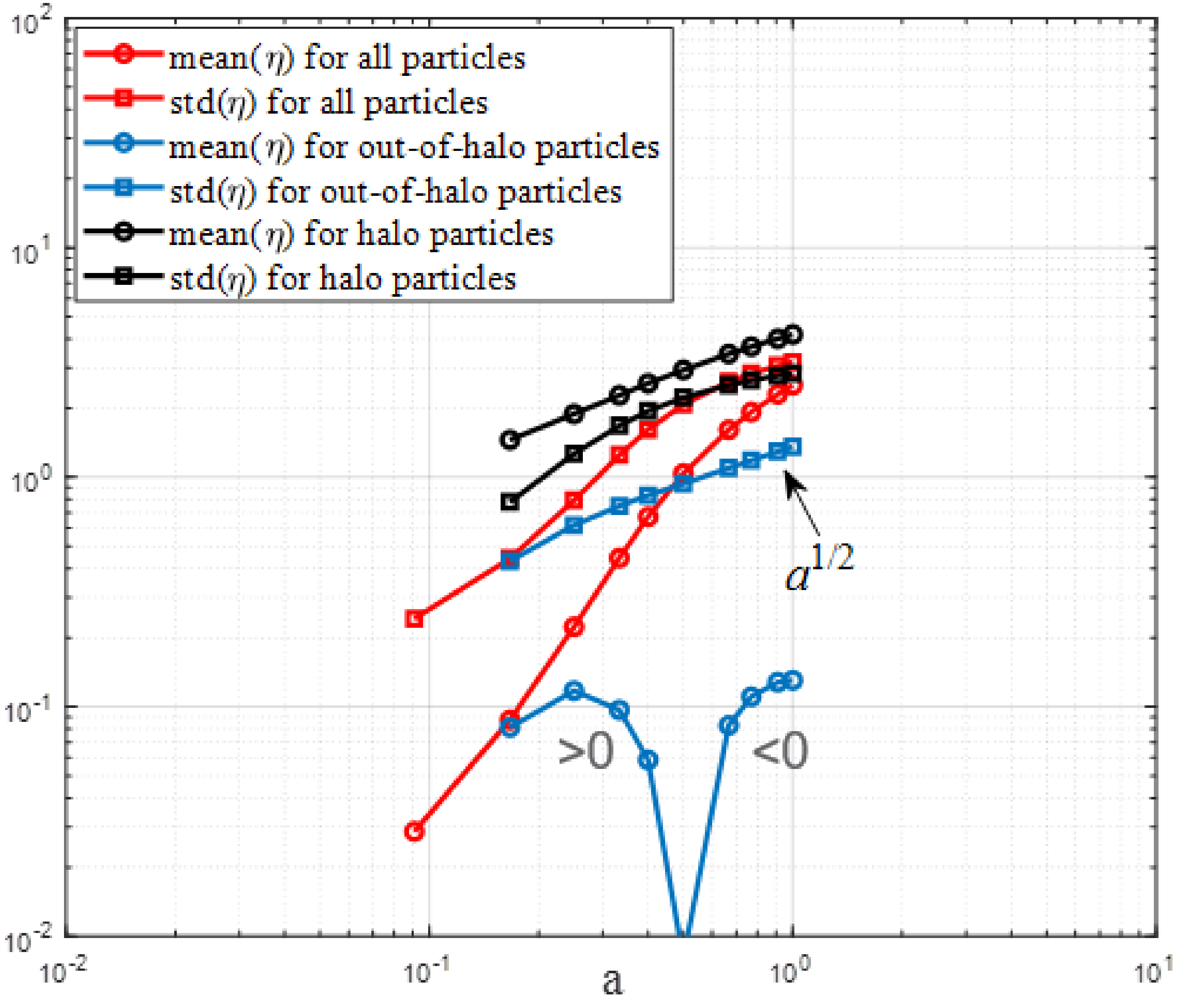

The variation of mean and standard deviation of log-density with scale factor a.

Two-point statistical measures of density field

Defining two-point density correlation function from radial distribution function g(r) in statistic mechanics, a quantity to measure the averaged particle density from an arbitrary reference particle:

$$dN_p = g(r)\frac{N_p}{V}4\pi r^2 dr$$

N_p/V

mean number density of particles in entire system

$$\int_0^\infty g(r)4\pi r^2 dr = \frac{N_p - 1}{N_p}V$$

$$\xi(r) = \langle \delta(\mathbf{x})\delta(\mathbf{x}+\mathbf{r})\rangle = g(r) - 1$$

$$\int_0^\infty \xi(r,a)4\pi r^2 dr = -V/N_p < 0$$

Correlation cannot be positive on all scales

Two length scales can be defined from density correlation:

$$l_{\delta 0}(a) = \int_0^\infty \xi(r,a)dr \qquad l_{\delta 1}^2(a) = \int_0^\infty \xi(r,a)rdr$$

On large scale, transverse velocity correlation can be well modelled by exponential function:

$$T_2(r,a) = a_0 u^2 \exp\left(-\frac{r}{r_2}\right) \propto a \qquad a_0(u/u_0)^2 = 0.45a$$

$$r_2 \approx 21.4\,Mpc/h$$

Redshift-independent length scale, might be related to the size of sound horizon

Total velocity correlation

$$R_2(r,a) = \langle \mathbf{u}\cdot\mathbf{u}'\rangle = 2R(r) = a_0 u^2 \exp\left(-\frac{r}{r_2}\right)\left(3 - \frac{r}{r_2}\right)$$

$$\delta \approx \eta = -\frac{\nabla\cdot\mathbf{u}}{aHf(\Omega_m)}$$

Linear perturbation theory on large scale:

Modeling density correlation on large scale:

$$\xi(r,a) = \frac{1}{(aHf(\Omega_0))^2}\cdot\frac{a_0 u^2}{r r_2}\exp\left(-\frac{r}{r_2}\right)\left[\left(\frac{r}{r_2}\right)^2 - 7\left(\frac{r}{r_2}\right) + 8\right]$$

Specific potential/kinetic energy from density correlation function

In statistical mechanics, potential energy of any system with particles interacting via a pairwise potential $V_g(r)$ can be related to the radial distribution function g(r):

$$PE = \frac{2\pi\rho_0}{m_p^2}\int_0^\infty r^2\left[g(r)-1\right]V_g(r)\,dr$$

$$P_y(a) = -\frac{2\pi G\rho_0}{a}\int_0^\infty \xi(r,a)\,r\,dr = -\frac{3H_0^2 l_{\delta 1}^2}{4a} < 0$$

Cosmic energy equation

$$\frac{\partial\left(K_p + P_y\right)}{\partial t} + H\left(2K_p + P_y\right) = 0$$

$$K_p = a^{-2}\int_0^a aP_y\,da - P_y \Rightarrow K_p = \frac{3}{4}H_0^2 a^{-1}\left(l_{\delta 1}^2 - a^{-1}\int_0^a l_{\delta 1}^2\,da\right)$$

Power-law evolution and rate of energy cascade ε_u:

$$K_p = -\varepsilon_u t \quad P_y = \frac{7}{5}\varepsilon_u t \Rightarrow l_{\delta 1}^2(a) = \int_0^\infty \xi(r,a)\,r\,dr = -\frac{56}{45}\frac{\varepsilon_u}{H_0^3}a^{5/2}$$

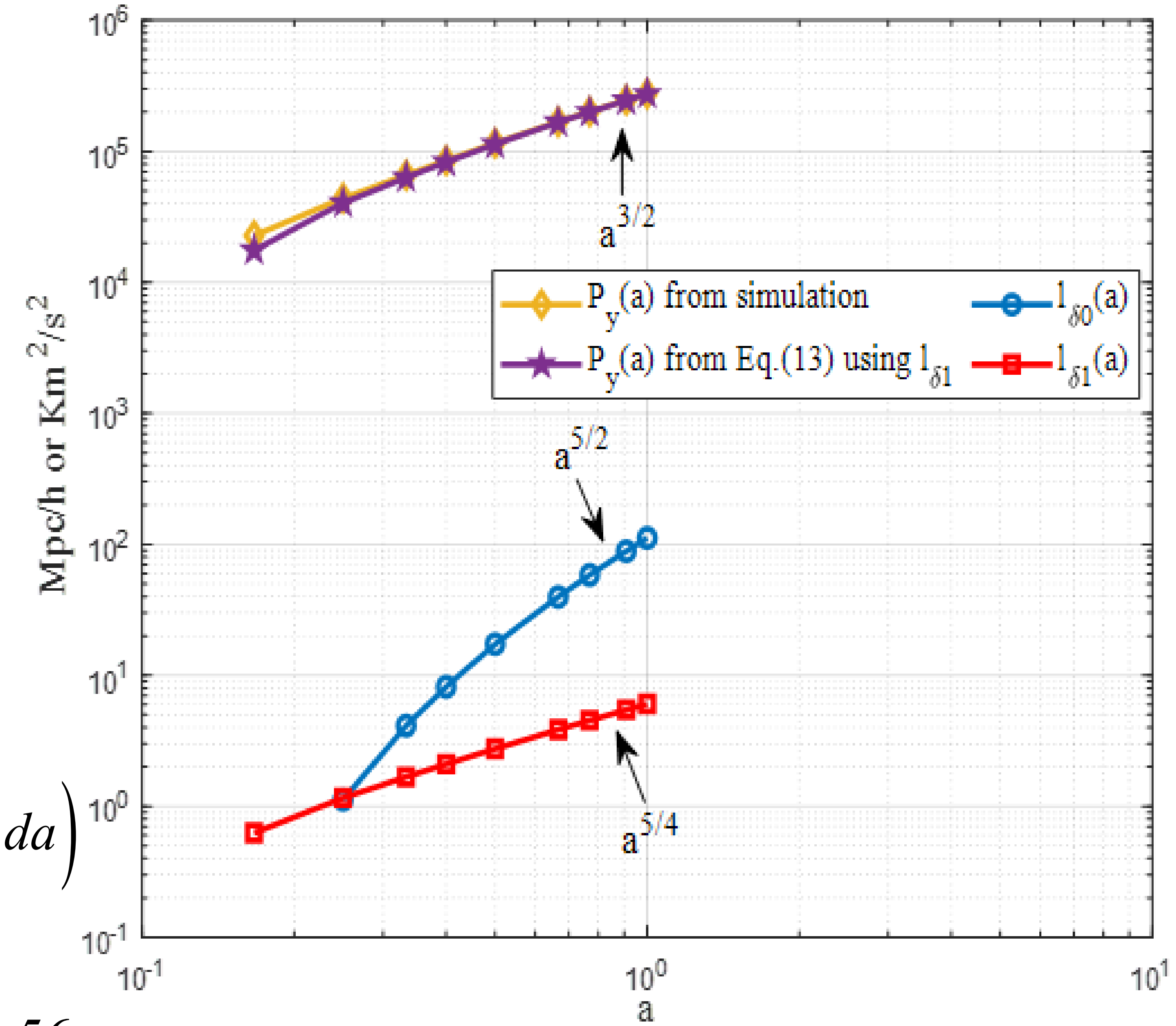

The variation of two comoving correlation lengths with scale factor a.

Density spectrum/dispersion functions and real space distribution of density fluctuation

Correlation and spectrum form Fourier pair:

$$E_\delta(k,a)=\frac{2}{\pi}\int_0^\infty \xi(r,a)\,kr\sin(kr)\,dr$$

$$\xi(r,a)=\int_0^\infty E_\delta(k,a)\frac{\sin(kr)}{kr}dk$$

Matter spectrum function:

$$P_\delta(k,a)=2\pi^2 E_\delta(k,a)/k^2$$

The power per logarithmic interval:

$$\Delta_\delta^2(k,a)=E_\delta(k,a)k$$

Density dispersion function (the variance of the density fluctuation on scale r):

$$\sigma_\delta^2(r,a)=\int_{-\infty}^{\infty}E_\delta(k,a)W(kr)^2\,dk$$

First order spherical Bessel function of the first kind

Window function when smoothed with a filter of size r

$$W(x\equiv kr) \qquad W(x)=\frac{3}{x^3}\left[\sin(x)-x\cos(x)\right]=3\frac{j_1(x)}{x}$$

$$\xi(2r)=\frac{1}{72r^2}\frac{\partial}{\partial r}\left(\frac{1}{r^2}\frac{\partial}{\partial r}\left(r^3\frac{\partial}{\partial r}\left(\sigma_\delta^2(r)r^4\right)\right)\right)$$

$$E_{\delta r}(r)=-\frac{\partial\sigma_\delta^2(r)}{\partial r}$$

The real-space distribution of density fluctuation in scales [r, r+dr]

Modeling density dispersion function on large scale:

$$\sigma_\delta^2(r)=\frac{1}{\left(aHf(\Omega_0)\right)^2}\cdot\frac{9a_0u^2}{2r^2}\left\{3\left(\frac{r_2}{r}\right)^4+\left(\frac{r_2}{r}\right)^2-\exp\left(-\frac{2r}{r_2}\right)\left[1+\left(\frac{r_2}{r}\right)^2\right]\left[3\left(\frac{r_2}{r}\right)^2+6\left(\frac{r_2}{r}\right)+4\right]\right\}$$

Density correlation function (simulations & models)

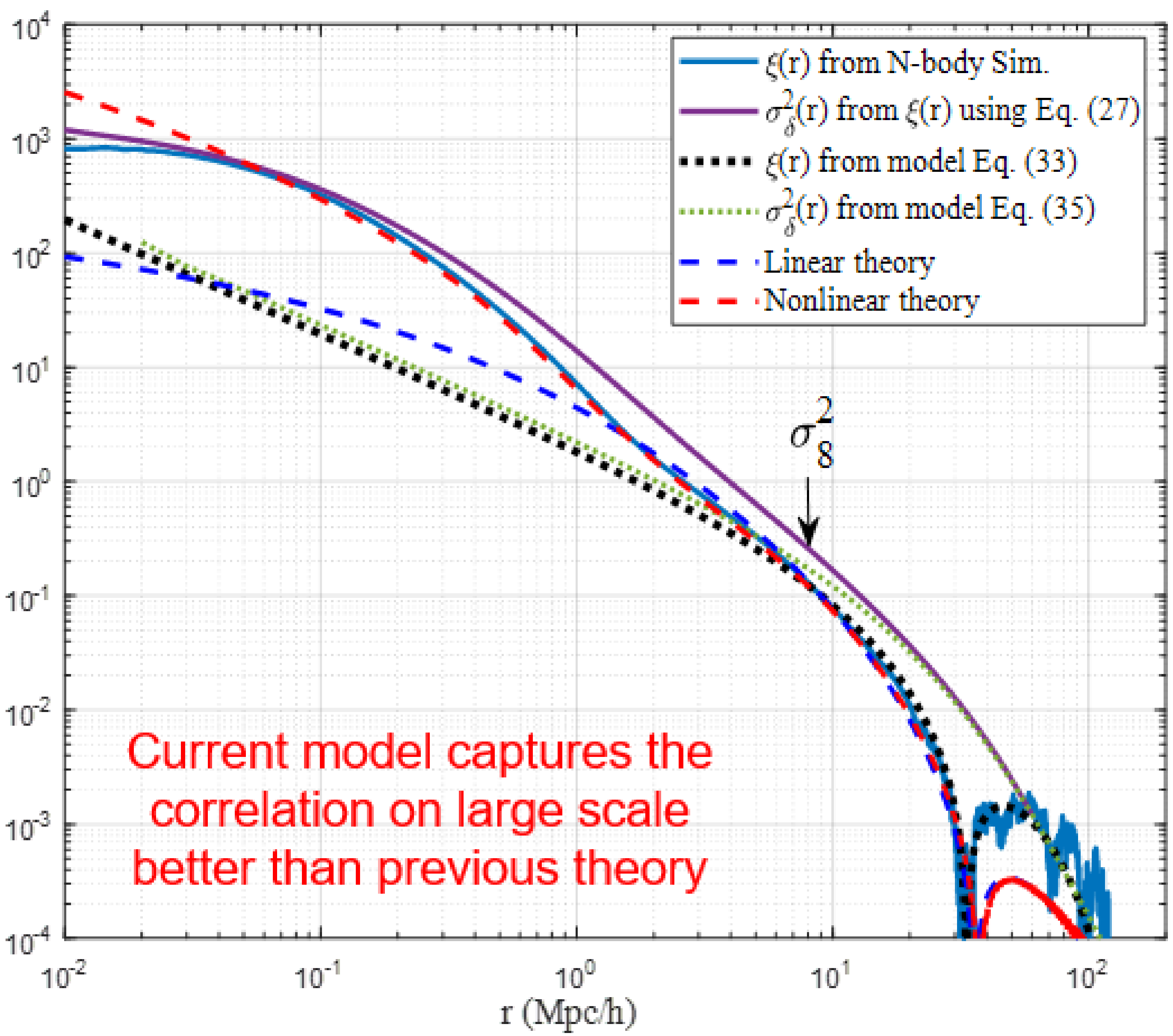

Density correlation function (solid blue) varying with scale r at z=0.

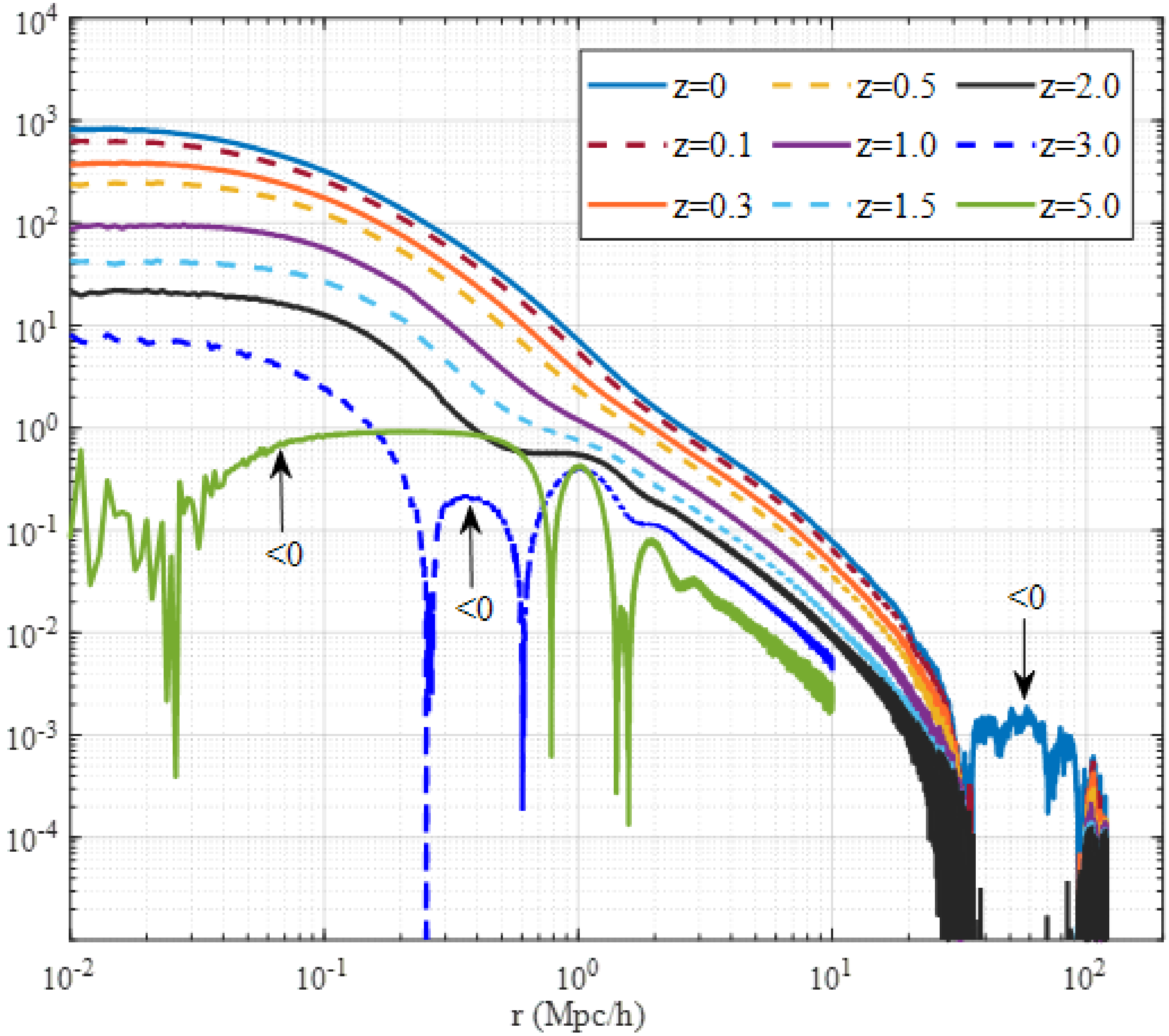

Density correlation function varying with scale r at different redshifts.

Density correlation and spectrum functions (simulation & models)

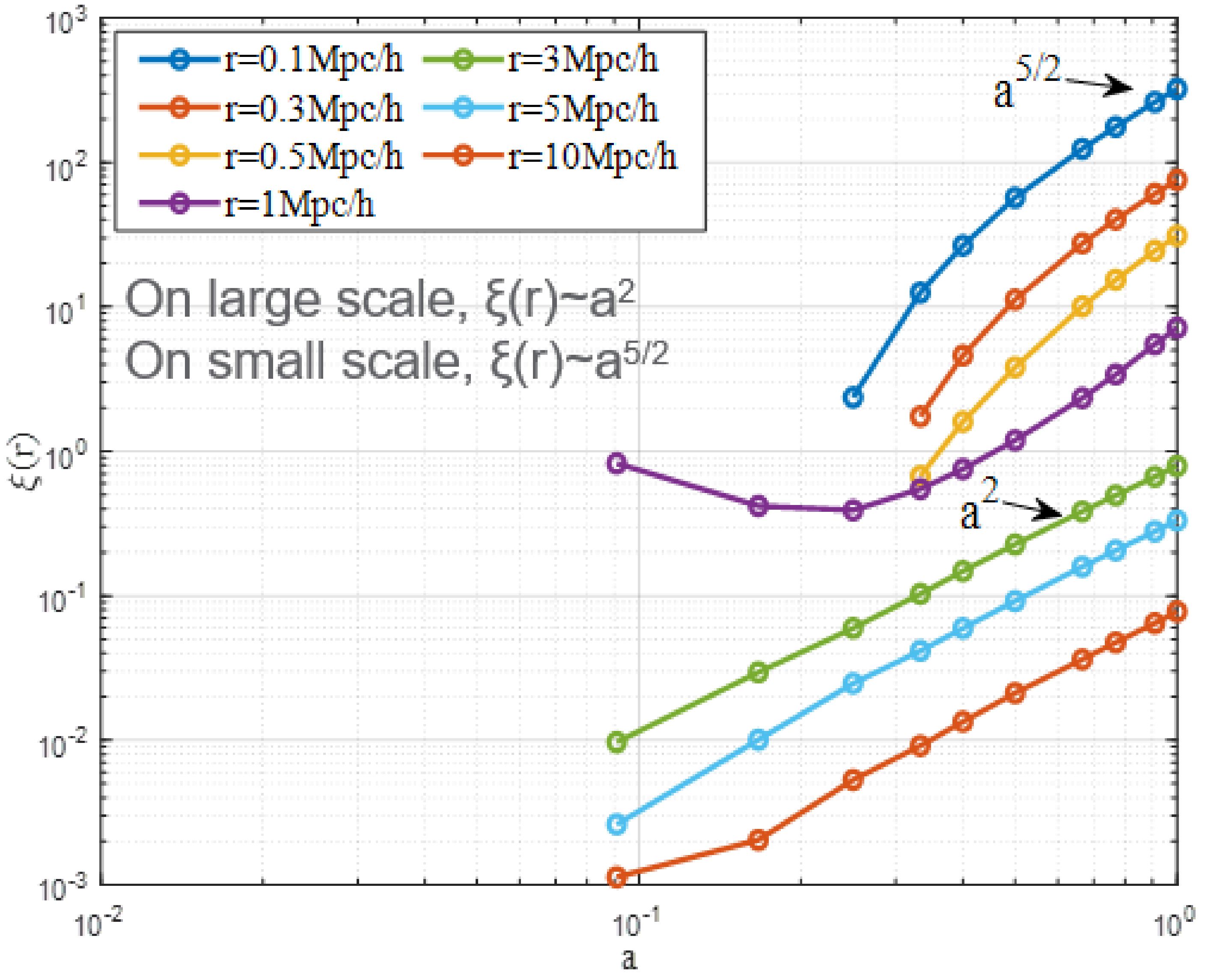

Two-point second order density correlation varying with scale factor a.

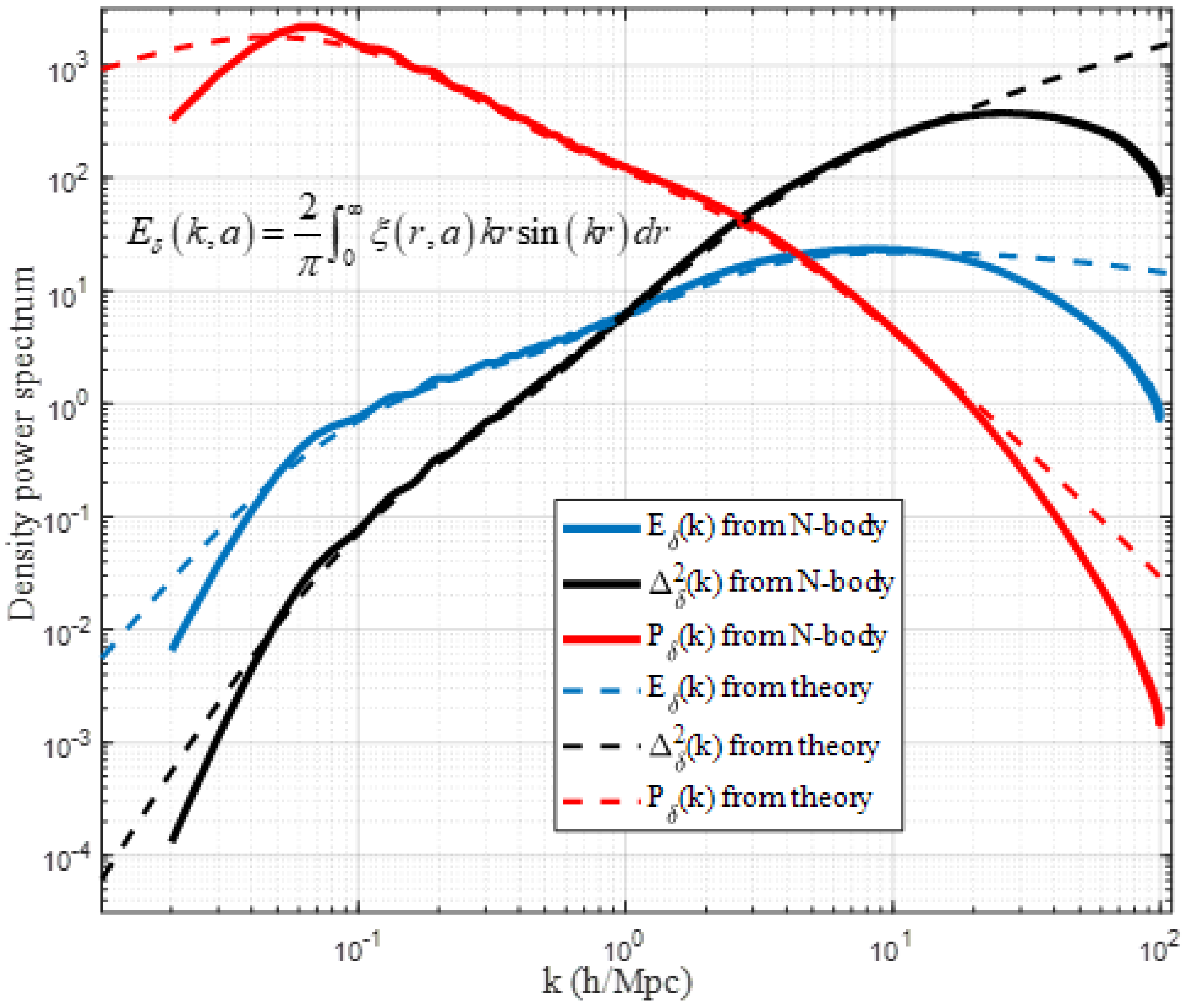

Without projection, density power spectrum can be obtained from Fourier transform of correlation.

Density dispersion function and distribution of density fluctuation

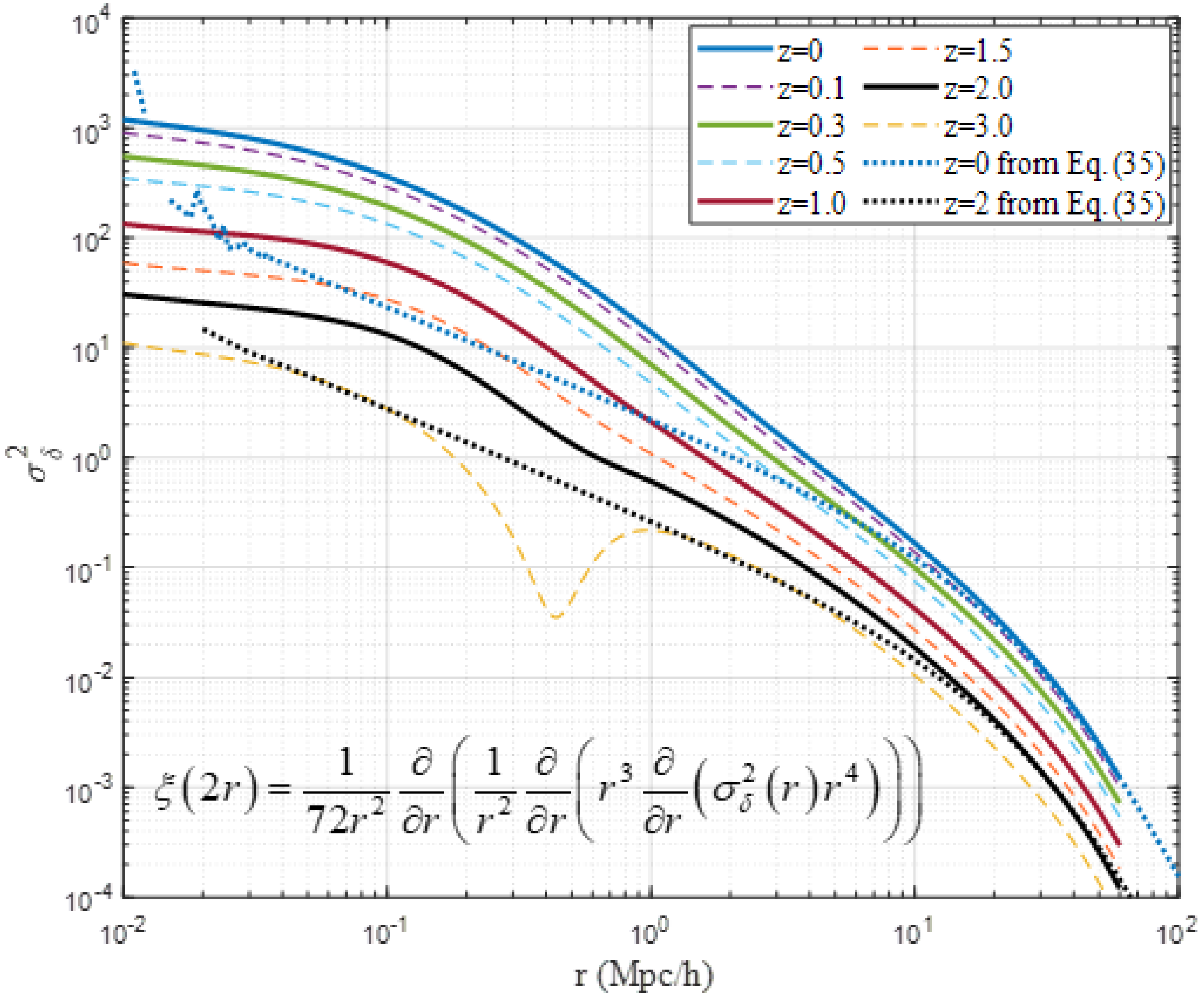

Density dispersion function obtained from density correlation and compared with models.

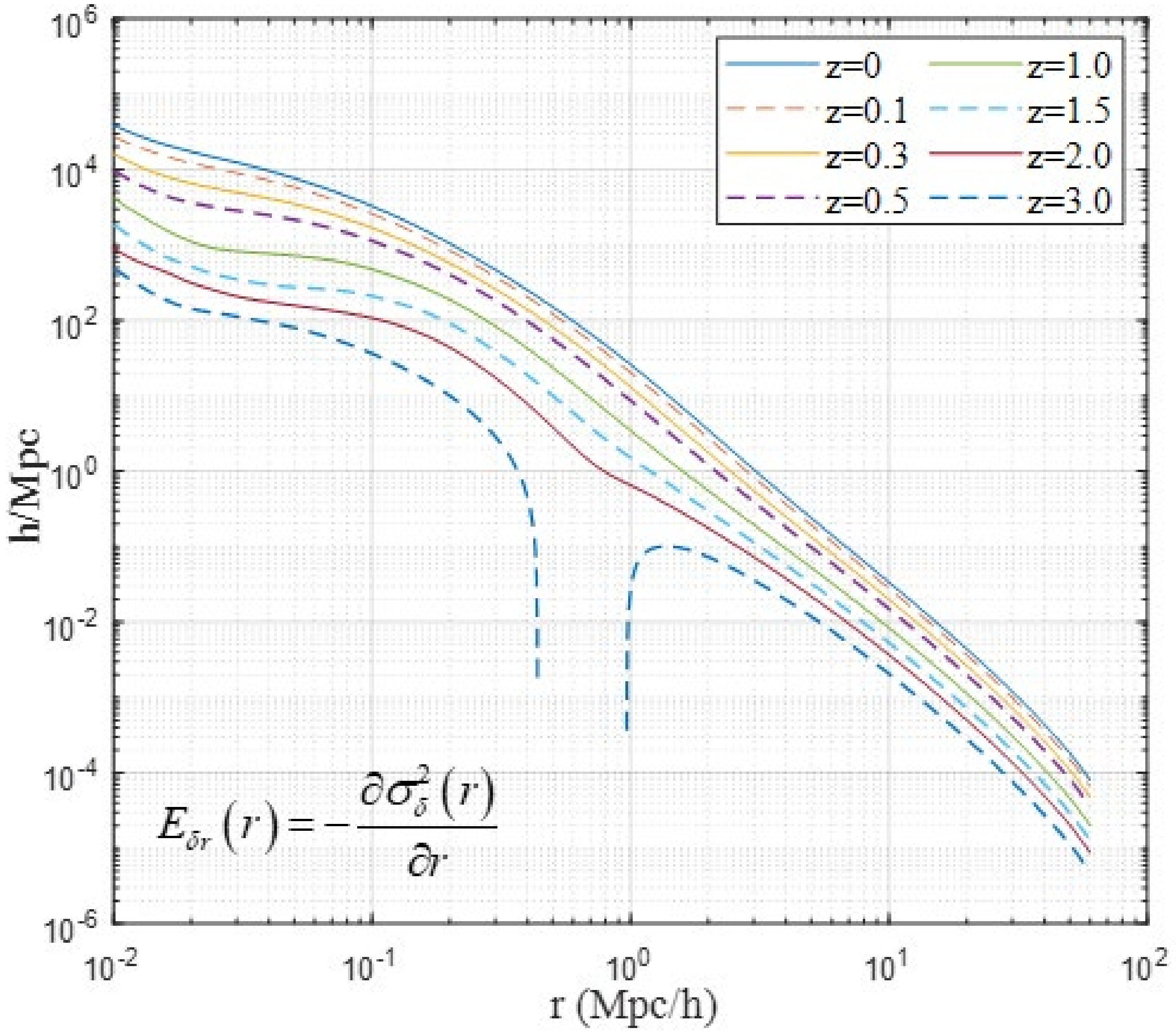

Distribution of density fluctuation on scale r obtained from density dispersion function

Characterizing distributions of velocity fields

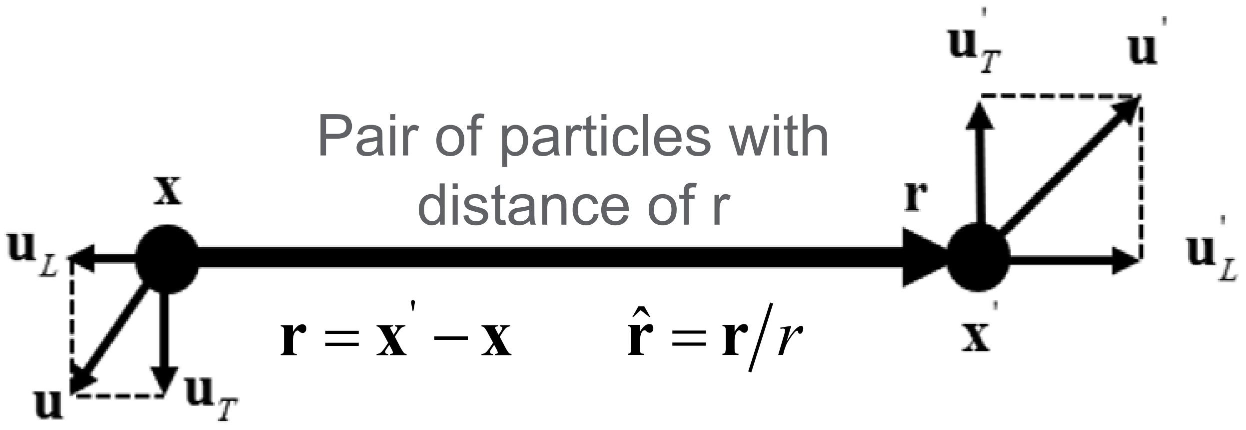

Longitudinal velocity:	Transverse velocity:
$u_L = \mathbf{u} \cdot \hat{\mathbf{r}} = u_i \hat{r}_i$	$\mathbf{u}_T = -(\mathbf{u} \times \hat{\mathbf{r}} \times \hat{\mathbf{r}})$
$u'_L = \mathbf{u}' \cdot \hat{\mathbf{r}} = u'_i \hat{r}_i$	$\mathbf{u}'_T = -(\mathbf{u}' \times \hat{\mathbf{r}} \times \hat{\mathbf{r}})$

Velocity difference or Pairwise velocity: $\Delta u_L = u'_L - u_L$

Velocity sum: $\sum u_L = u'_L + u_L$

We focus on the distribution of seven types of velocities:

Scale-dependent velocities (dependent on r):

- Longitudinal velocity: u'_L and u_L
- Pairwise velocity: $\Delta u_L = u'_L - u_L$
- Velocity sum: $\sum u_L = u'_L + u_L$

Based on halo-based non-projection approach,

Redshift-dependent velocities (dependent on z):

- Velocity of all particles in entire system: $\mathbf{u}_p$
- Velocity of all halo particles: $\mathbf{u}_{hp}$
- Velocity of all out-of-halo particles: $\mathbf{u}_{op}$
- Velocity of all halos: $\mathbf{u}_h$

Redshift dependence of velocity distributions

The scale and redshift variation can be studied by Introducing generalized Kurtosis:

$$K_n\left(\Delta u_L, r\right)=\frac{\left\langle\left(\Delta u_L-\left\langle\Delta u_L\right\rangle\right)^n\right\rangle}{\left\langle\left(\Delta u_L-\left\langle\Delta u_L\right\rangle\right)^2\right\rangle^{n/2}}=\frac{S_n^{cp}\left(\Delta u_L, r\right)}{S_2^{cp}\left(\Delta u_L, r\right)^{n/2}}$$

The central moment of order *n*:

$$S_n^{cp}\left(\Delta u_L, r\right)=\left\langle\left(\Delta u_L-\left\langle\Delta u_L\right\rangle\right)^n\right\rangle$$

The *n*th order longitudinal structure function:

$$S_n^{lp}\left(r\right)=\left\langle\left(\Delta u_L\right)^n\right\rangle=\left\langle\left(u_L^{'}-u_L\right)^n\right\rangle$$

- All velocities are initially Gaussian.
- Velocity distribution of halo particles deviates from Gaussian much faster than out-of-halo particles due to stronger gravitational interaction in halos.
- All velocities become non-Gaussian with time to maximize system entropy

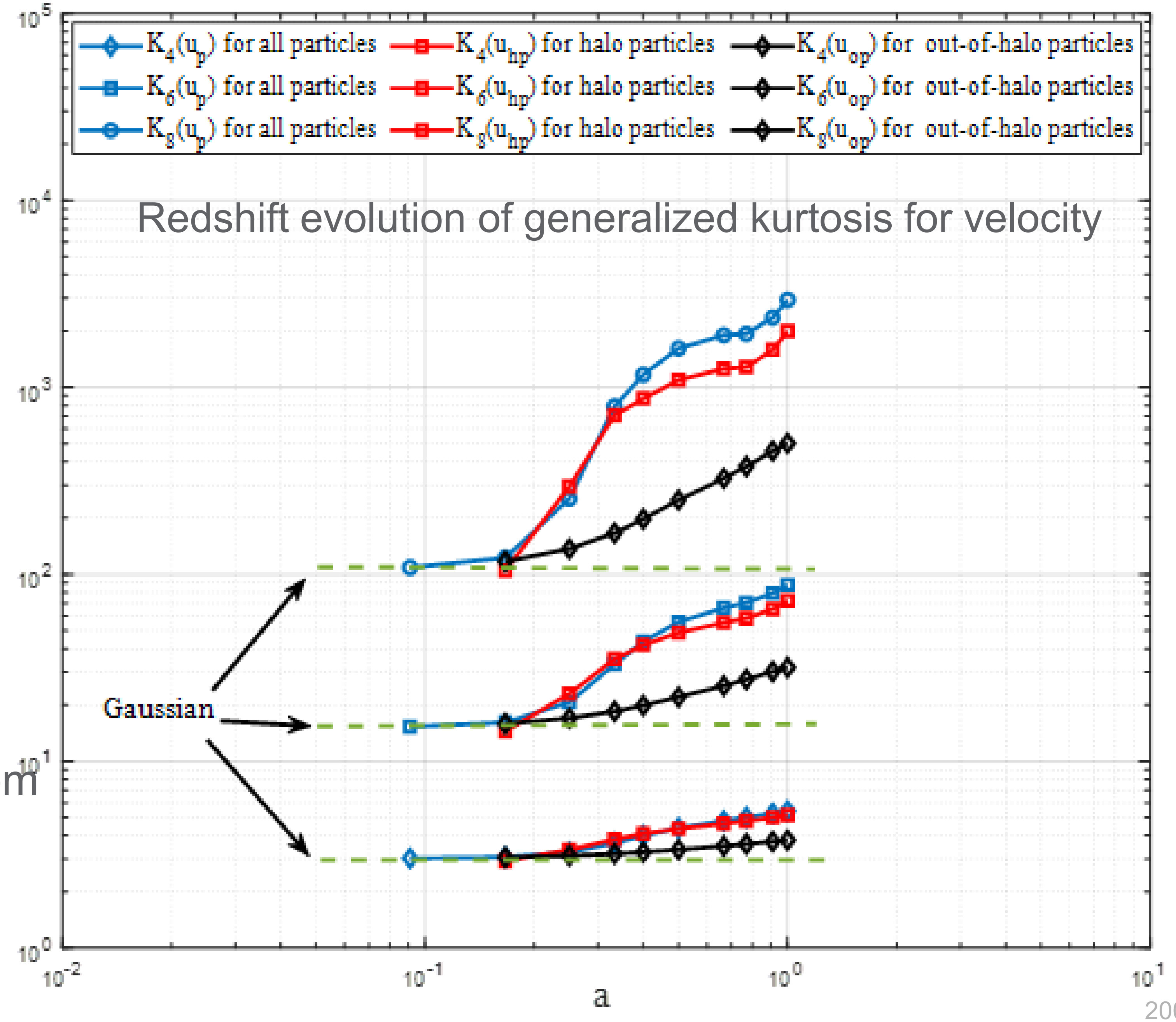

Scale-dependence of velocity distributions

- Even order generalized kurtosis (4th, 6th, and 8th order) at z=0.
- Velocity of fully developed dark matter flow is never Gaussian on any scale due to long-range gravity despite that they can be initially Gaussian.
- For incompressible flow with short range force, distribution is nearly Gaussian on large scale and non-Gaussian on small scale due to viscous force.
- On small scale, distribution of ΣuL approaches the distribution of uL with ρ_L=0.5.
- On large scale, distribution of ΣuL approaches the distribution of ΔuL with ρ_L=0.

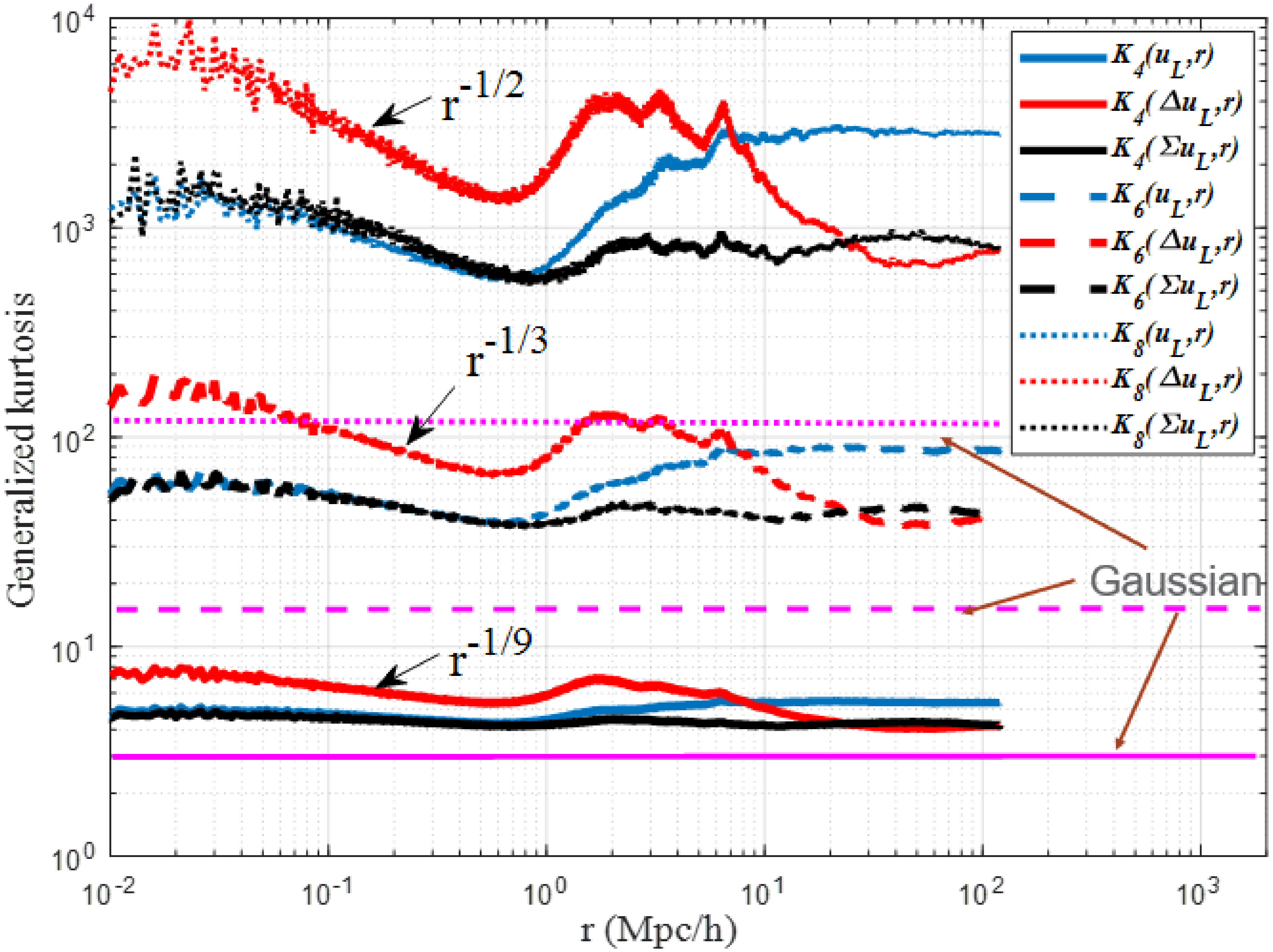

Scale-dependence of velocity distributions

- On both small and large scales, generalized kurtosis approaches constant such that there exist unique (limiting) probability distributions that are independent of scale r.
- While on the intermediate scale around 1Mpc/h, all three velocity distributions exhibit the greatest value of generalized kurtosis of different order.
- Third order kurtosis (skewness) vanishes on both small and large scales, where distributions are symmetric.
- The negative skewness on the intermediate scale (distribution skews toward positive side) can be an important signature of inverse cascade of kinetic energy.

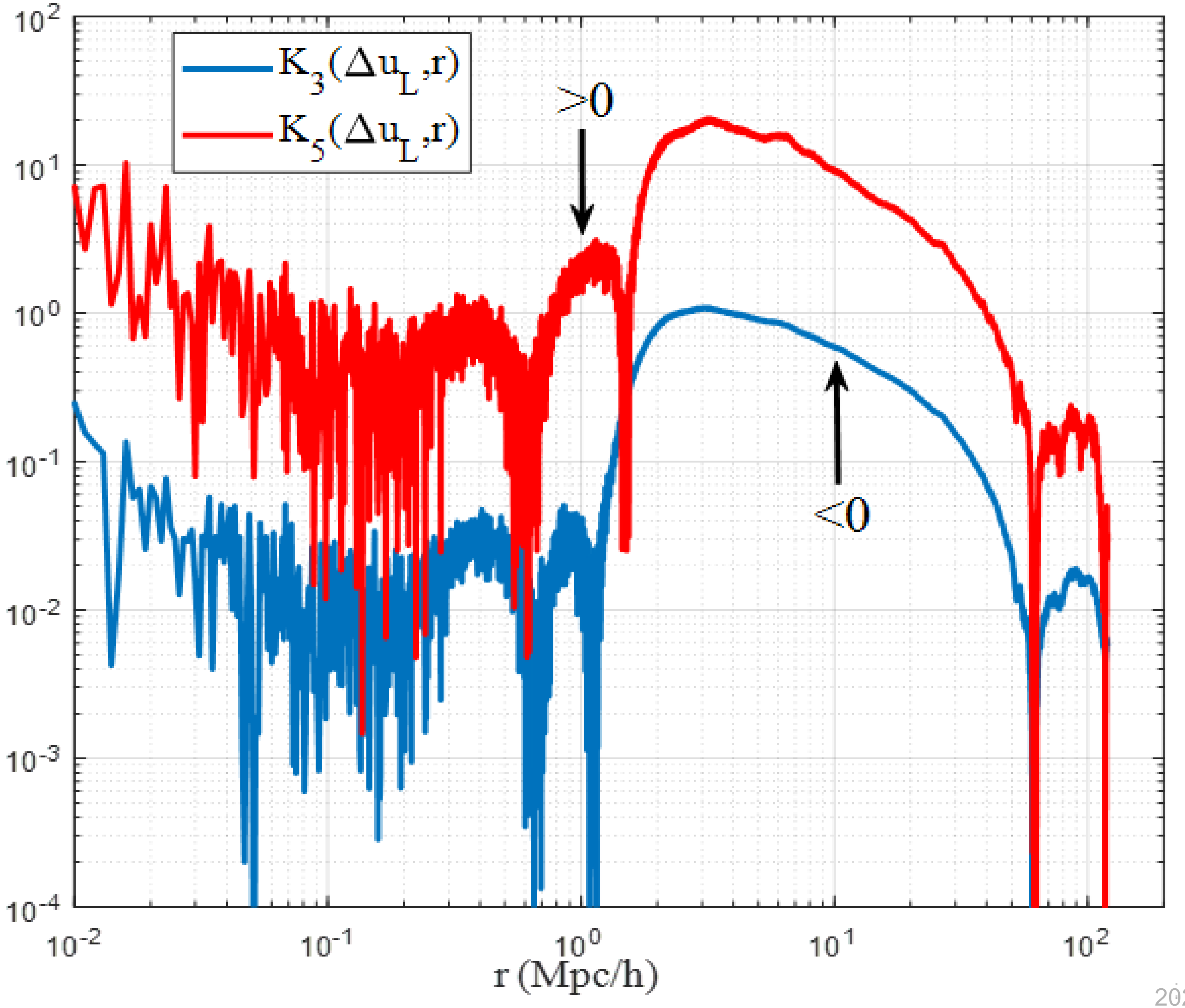

First moment of velocity fields and pair conservation equation

Pair conservation equation relates the pairwise velocity with density correlation

$$\frac{\langle \Delta u_L \rangle}{Har} = -\frac{\left(1+\bar{\xi}(r,a)\right)}{3\left(1+\xi(r,a)\right)} \frac{\partial \ln\left(1+\bar{\xi}(r,a)\right)}{\partial \ln a}$$

For large scale in linear regime, average correlation

$\bar{\xi} \ll 1$ and $\partial \ln \bar{\xi} / \partial \ln a = 2$

$$\frac{\langle \Delta u_L \rangle}{Har} = -\frac{2\bar{\xi}(r,a)\left(1+\bar{\xi}(r,a)\right)}{3\left(1+\xi(r,a)\right)} \approx -\frac{2}{3}\bar{\xi}(r,a)$$

For small scale in non-linear regime,

$\xi(r,a) \propto a^{\alpha} r^{\gamma}$ and $\partial \ln \bar{\xi} / \partial \ln a = \alpha$

Stable clustering hypothesis $\frac{\langle \Delta u_L \rangle}{Har} = -1$ $\Rightarrow$ $\alpha = \gamma + 3$

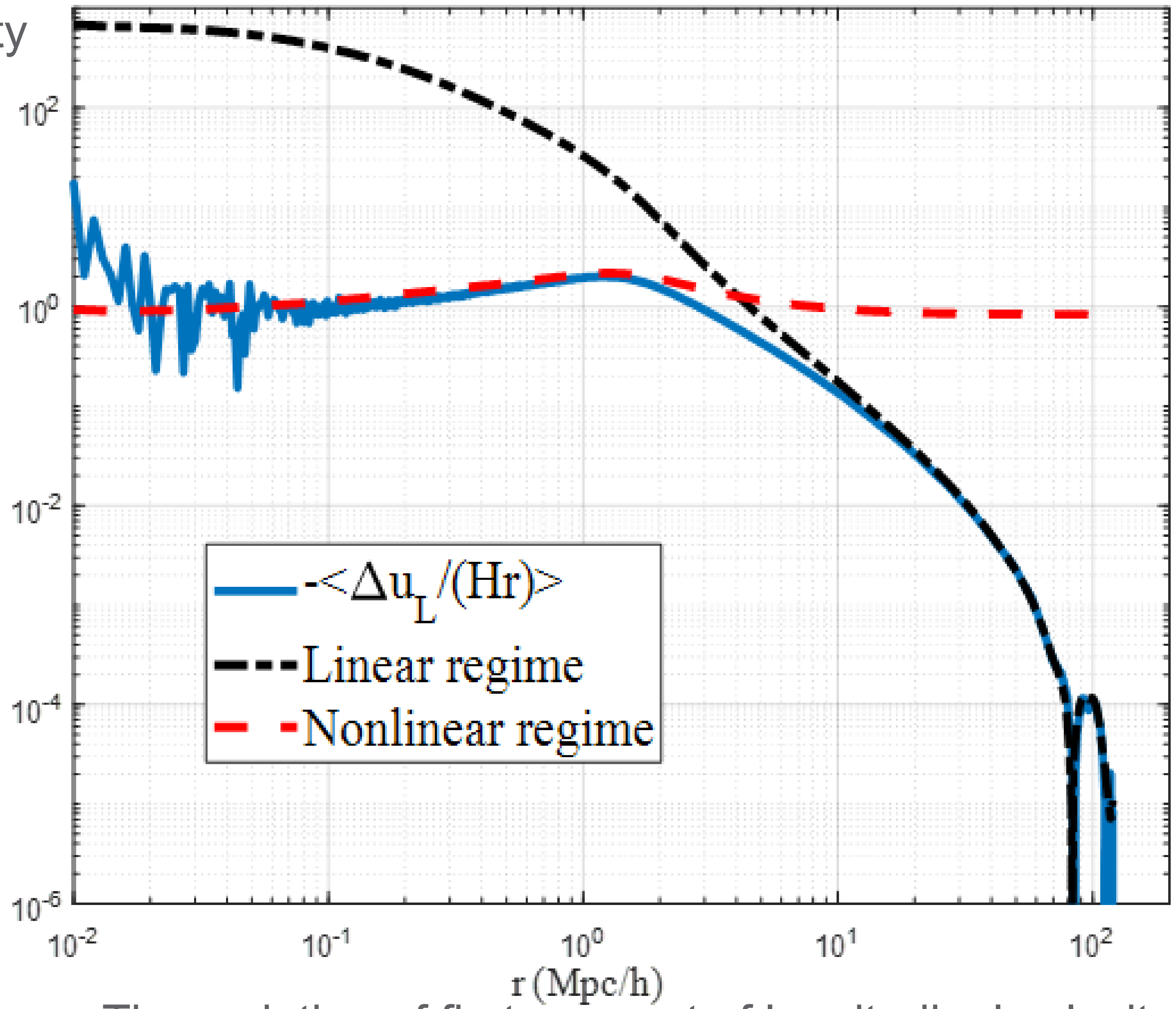

The variation of first moment of longitudinal velocity (mean pairwise velocity) with scale r

First moment of velocity fields

On small scale:

$$\langle \Delta u_L \rangle = -Har \quad \langle u_L \rangle = Har/2 \quad \langle \Sigma u_L \rangle = 0$$

A better relation to fit the simulation data:

$$\langle \Delta u_L \rangle = -Har - ua^{-5/3}\left(r/r_t\right)^{5/2}$$

On large scale:

$$\langle \Delta u_L \rangle = -\frac{2Ha}{r^2}\int_0^r \xi(y)\, y^2 dy$$

From pair conservation equation

$$R_2 = \langle \mathbf{u}\cdot\mathbf{u}' \rangle$$

Total velocity correlation

$$\langle \Delta u_L \rangle = \frac{2}{aHf(\Omega_0)}\frac{\partial R_2}{\partial r} = \frac{2a_0u^2}{aHr_2}\exp\left(-\frac{r}{r_2}\right)\left(\frac{r}{r_2}-4\right)$$

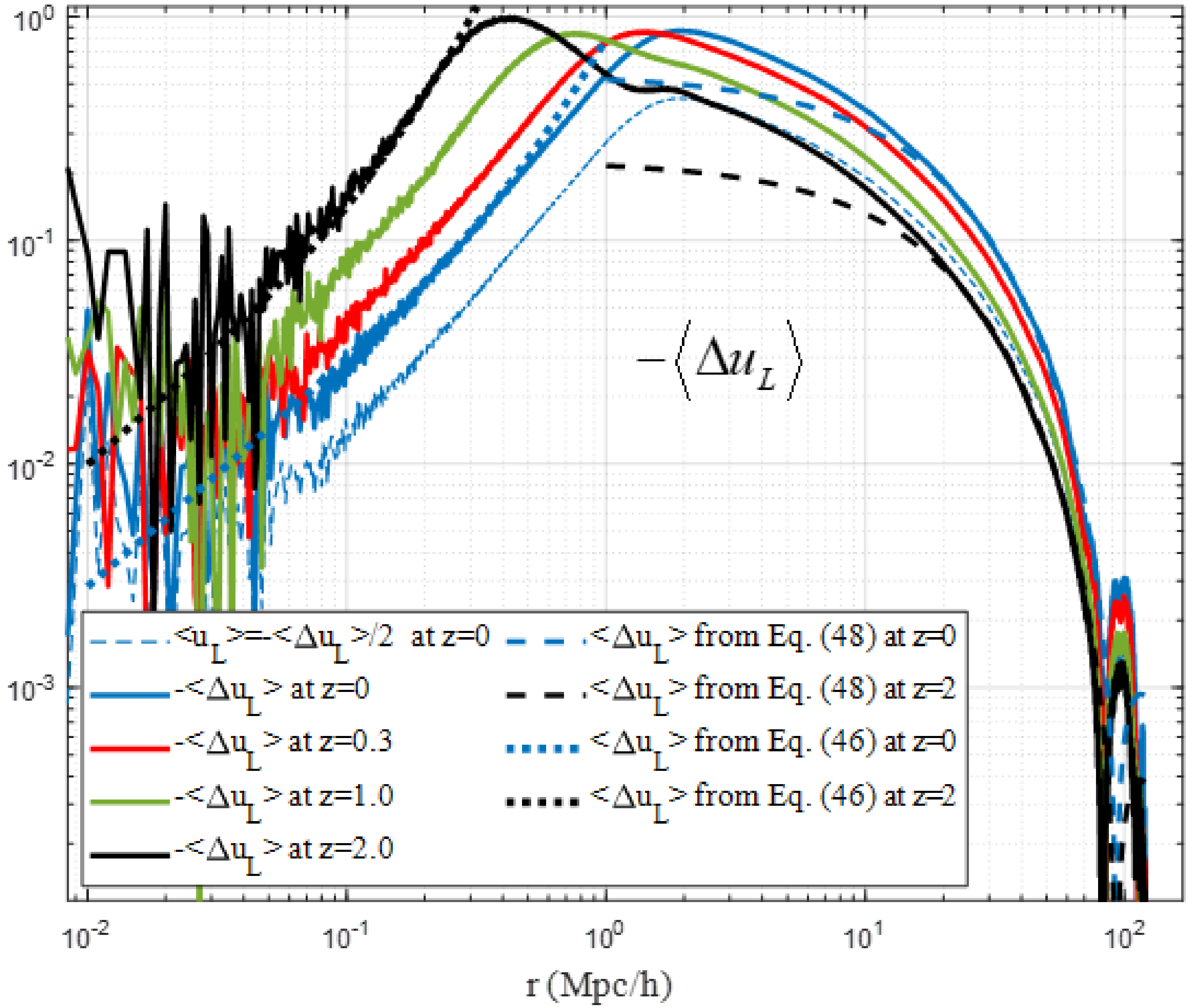

Mean velocity difference (pairwise velocity, normalized by u) varying with scale r at different redshift z

Second moment of velocity fields

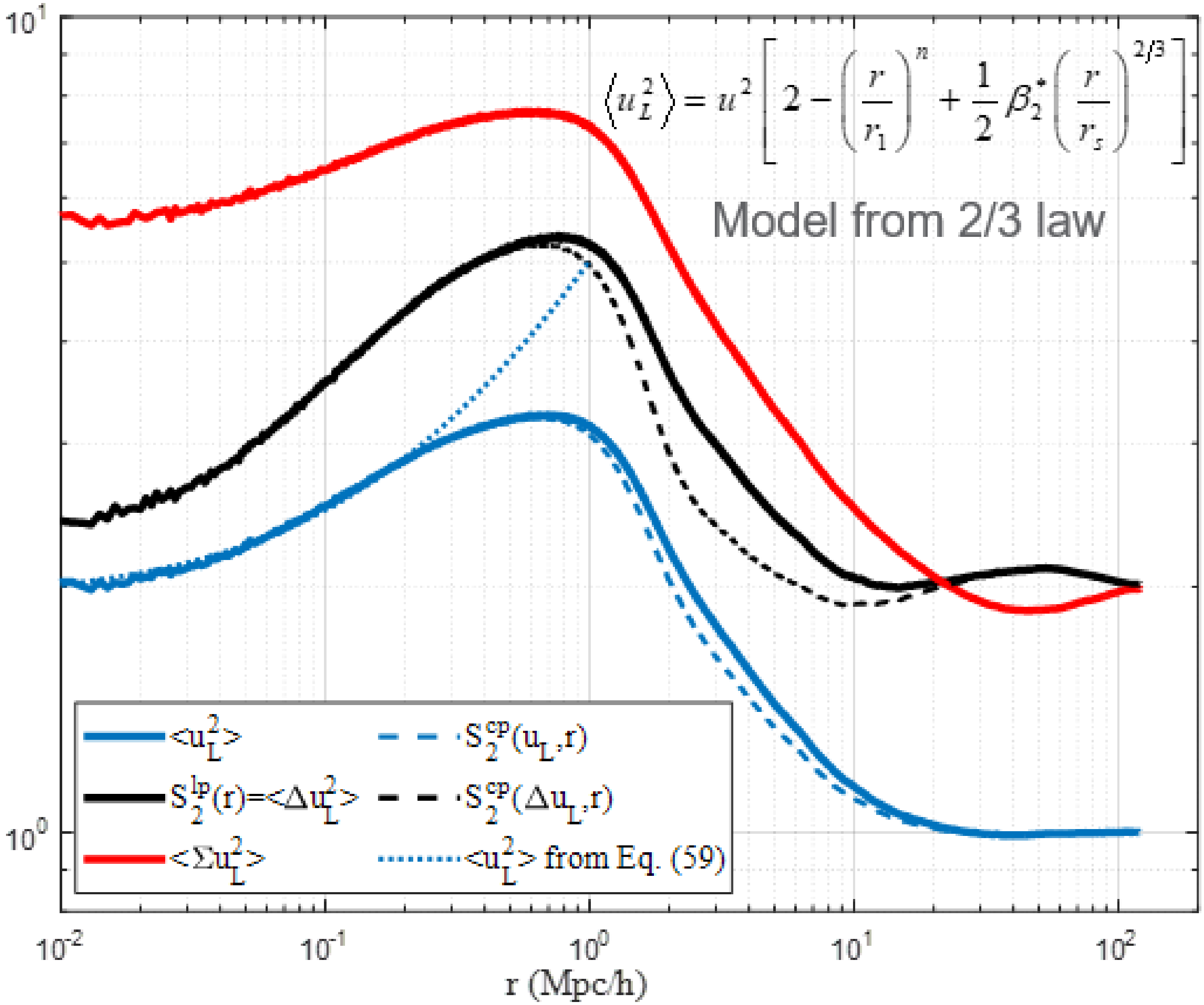

Increase of velocity dispersions with r for $r<r_t$ (pair of particles are more likely from same halos) is mostly due to the increase of velocity dispersion with halo size.

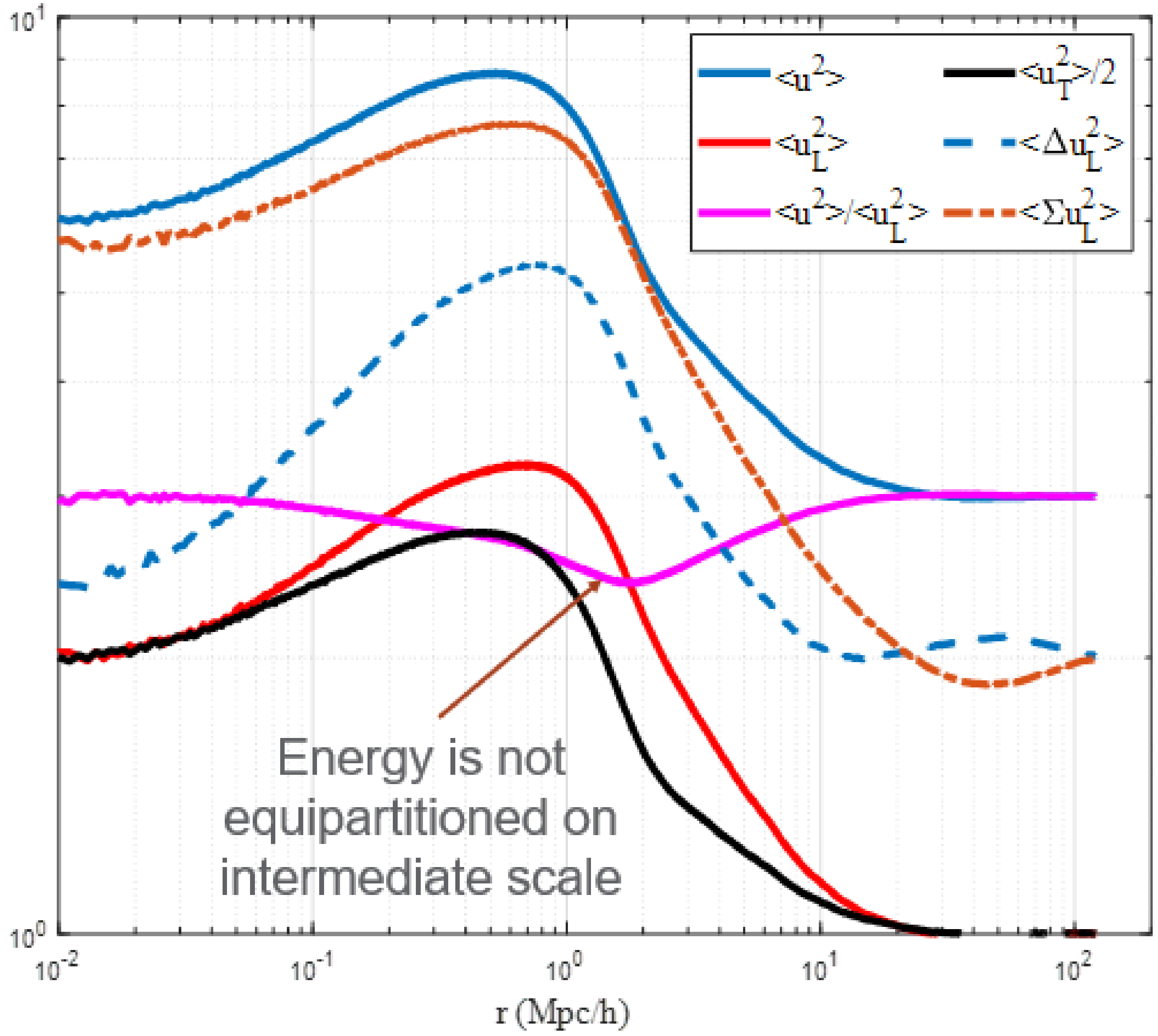

Second moment of velocity (normalized by u^2) varying with scale r at z=0

Second moment of pairwise velocity (pairwise dispersion) and the two-thirds law

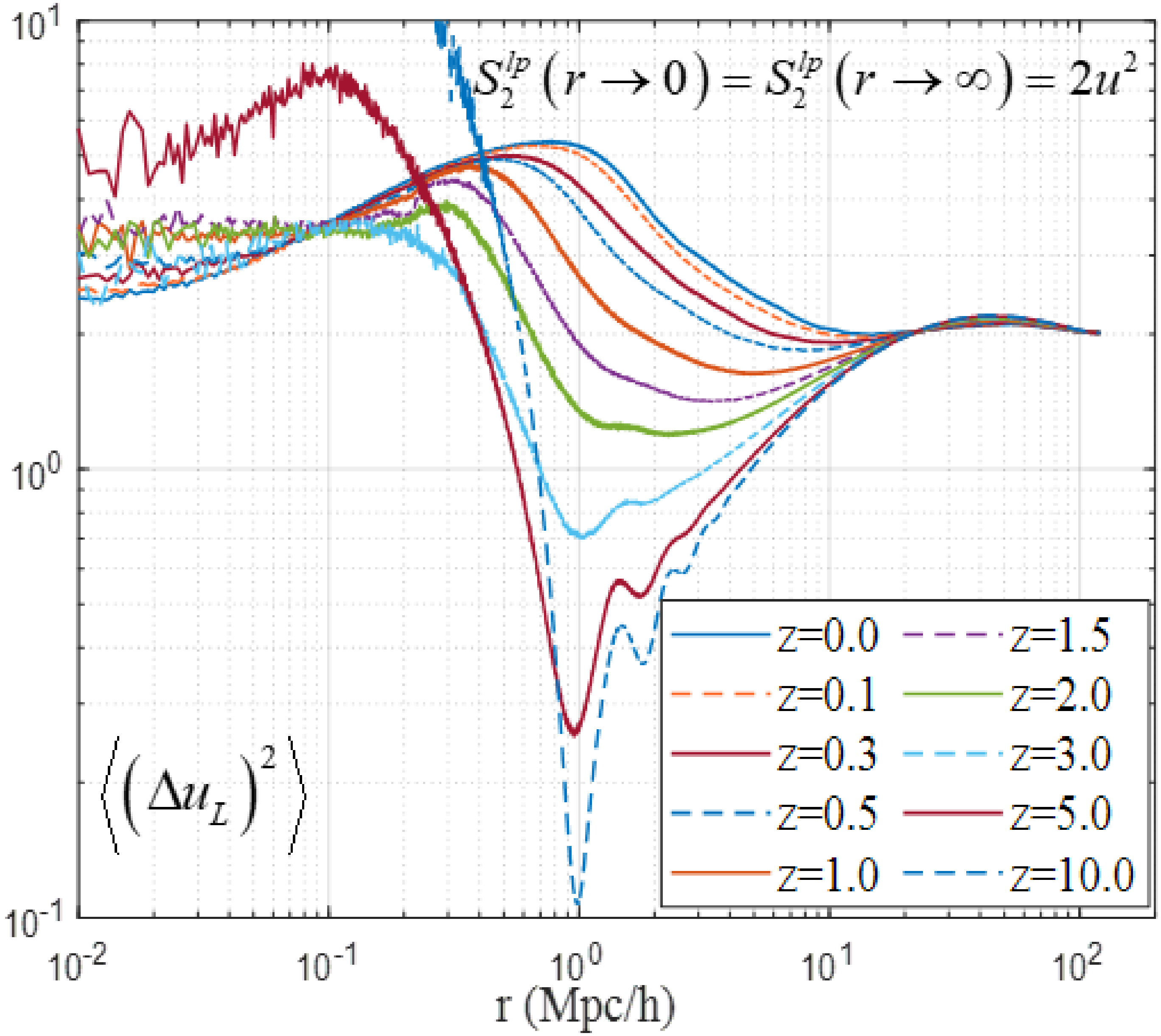

Second order longitudinal structure function (pairwise velocity dispersion)

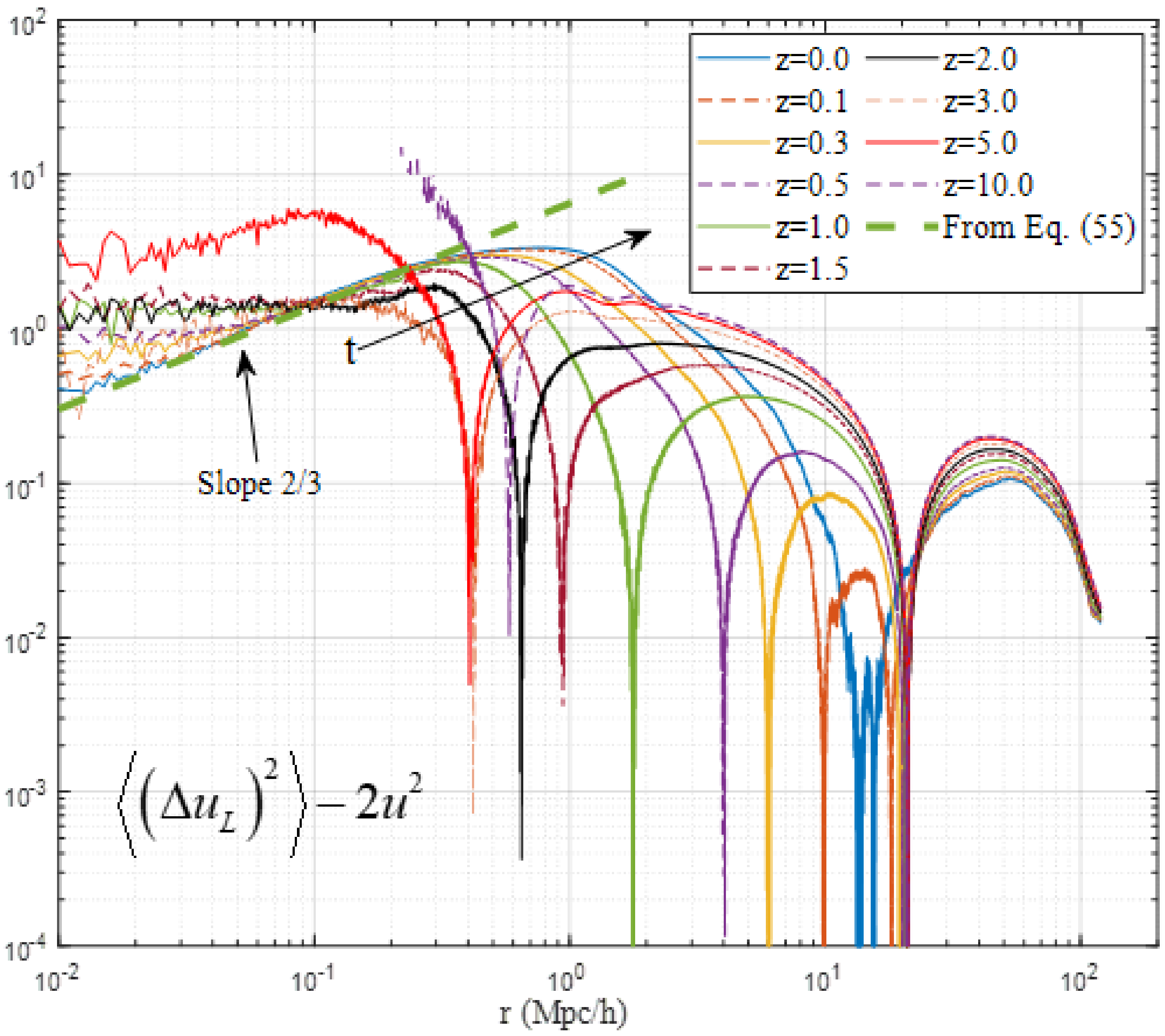

Reduced second order longitudinal structure function (pairwise velocity dispersion) and two-thirds law

Two-thirds law for higher even order structure functions and generalized stable clustering (GSCH)

Original scaling for incompressible flow does not apply for dark matter flow.

All even order reduced structure functions follow the same scaling of two-thirds law.

$$S_{2n}^{lp}(r) = u^{2n}\left[2^n K_{2n}(\Delta u_L, 0) + \beta_{2n}^*(r/r_s)^{2/3}\right]$$

$$r_s = -\frac{u_0^3}{\varepsilon_u} = \frac{4}{9}\frac{u_0}{H_0} = \frac{2}{3}u_0 t_0 \approx 1.58\,Mpc/h$$

$$-\varepsilon_u = \frac{3}{2}\frac{u_0^2}{t_0} = \frac{9}{4}u_0^2 H_0 = 4.6\times10^{-7}\,m^2/s^3$$

$$\beta_2^* = 9.5 \qquad \beta_4^* = 300 \qquad \beta_6^* = 2.25\times10^4$$

$$\beta_8^* = 2.75\times10^6 \qquad \beta_{2n}^* \approx 10^{1.826n-1.003}$$

All odd order structure functions follow linear law from generalized stable clustering hypothesis

$$S_{2n+1}^{lp}(r) = (2n+1)\,S_1^{lp}(r)\,S_{2n}^{lp}(r) \propto r^1$$

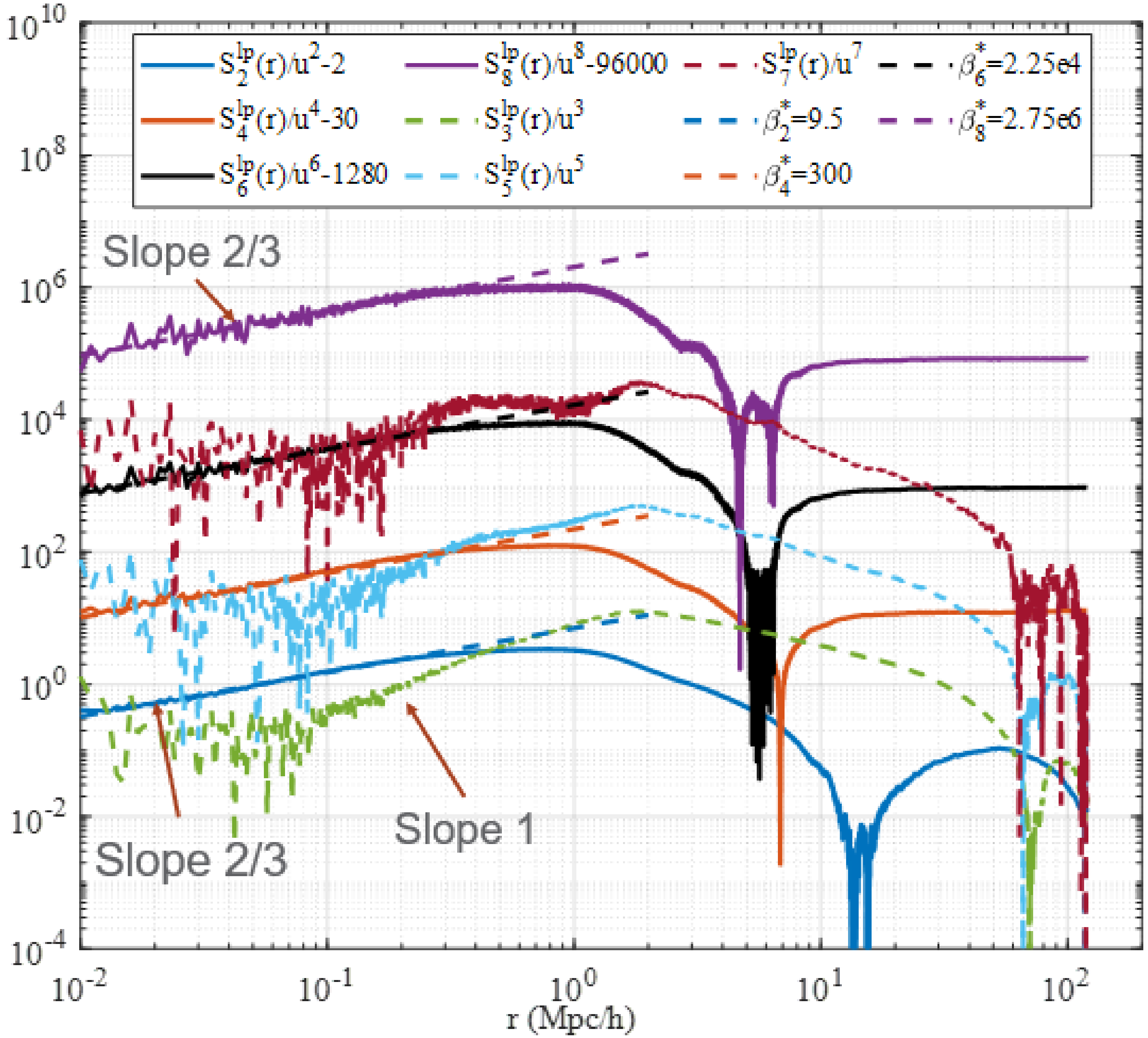

Comparison of velocity fields between incompressible and dark matter flow

Quantity	Incompressible flow	SG-CFD
$\langle u_L \rangle = \langle \mathbf{u} \cdot \hat{\mathbf{r}} \rangle$	0 for all scale r	$\lim_{r\to 0,\infty} \langle u_L \rangle = 0$, varying with r
$\langle u_L^2 \rangle$	u_0^2 for all scale r	$\lim_{r\to 0} \langle u_L^2 \rangle = 2u_0^2$, $\lim_{r\to\infty} \langle u_L^2 \rangle = u_0^2$
$\langle u_L^3 \rangle$	0 for all scale r	$\lim_{r\to 0,\infty} \langle u_L^3 \rangle = 0$, varying with r
PDF of u_L	Gaussian	Non-gaussian on all scales
$\langle \Delta u_L \rangle$	0 for all scale r	$\lim_{r\to 0,\infty} \langle \Delta u_L \rangle = 0$, varying with r
$\langle \Delta u_L^2 \rangle$	$\lim_{r\to 0} \langle \Delta u_L^2 \rangle = 0$, $\lim_{r\to\infty} \langle \Delta u_L^2 \rangle = u_0^2$	$\lim_{r\to 0} \langle \Delta u_L^2 \rangle = 2u_0^2$, $\lim_{r\to\infty} \langle \Delta u_L^2 \rangle = 2u_0^2$
$K_3(\Delta u_L)$	$\lim_{r\to 0} K_3(\Delta u_L) = -0.4$, $\lim_{r\to\infty} K_3(\Delta u_L) = 0$	$\lim_{r\to 0,\infty} K_3(\Delta u_L) = 0$, varying with r
$K_4(\Delta u_L)$	$\lim_{r\to 0} K_4(\Delta u_L) \approx 4$ (depends on Re), $\lim_{r\to\infty} K_4(\Delta u_L) = 3$ (Gaussian)	$\lim_{r\to 0} K_4(\Delta u_L) = 7.5$, $\lim_{r\to\infty} K_4(\Delta u_L) = 4.2$
$\langle \sum u_L \rangle$	0 on all scales	0 on all scales
$\langle \sum u_L^2 \rangle$	$\lim_{r\to 0} \langle \sum u_L^2 \rangle = 4u_0^2$, $\lim_{r\to\infty} \langle \sum u_L^2 \rangle = 2u_0^2$	$\lim_{r\to 0} \langle \Delta u_L^2 \rangle = 6u_0^2$, $\lim_{r\to\infty} \langle \Delta u_L^2 \rangle = 2u_0^2$

Modeling velocity distributions on small scale

- On small scale, velocities u_L and Σu_L should have the same limiting distribution.
- On small scale both should follow a X distribution to maximize system entropy.

Maximum entropy distribution:

$$X(v) = \frac{1}{2\alpha v_0} \frac{e^{-\sqrt{\alpha^2 + (v/v_0)^2}}}{K_1(\alpha)}$$

Shape parameter: α;
Velocity scale: v_0;

The mth order generalized kurtosis of X distribution:

$$K_m(X) = \left(\frac{2K_1(\alpha)}{K_2(\alpha)}\right)^{m/2} \frac{\Gamma((1+m)/2)}{\sqrt{\pi}} \cdot \frac{K_{(1+m/2)}(\alpha)}{K_1(\alpha)}$$

- The shape of velocity distribution changes with redshift z such that α is redshift-dependent.
- Kurtosis K_m is only dependent on α and also redshift-dependent

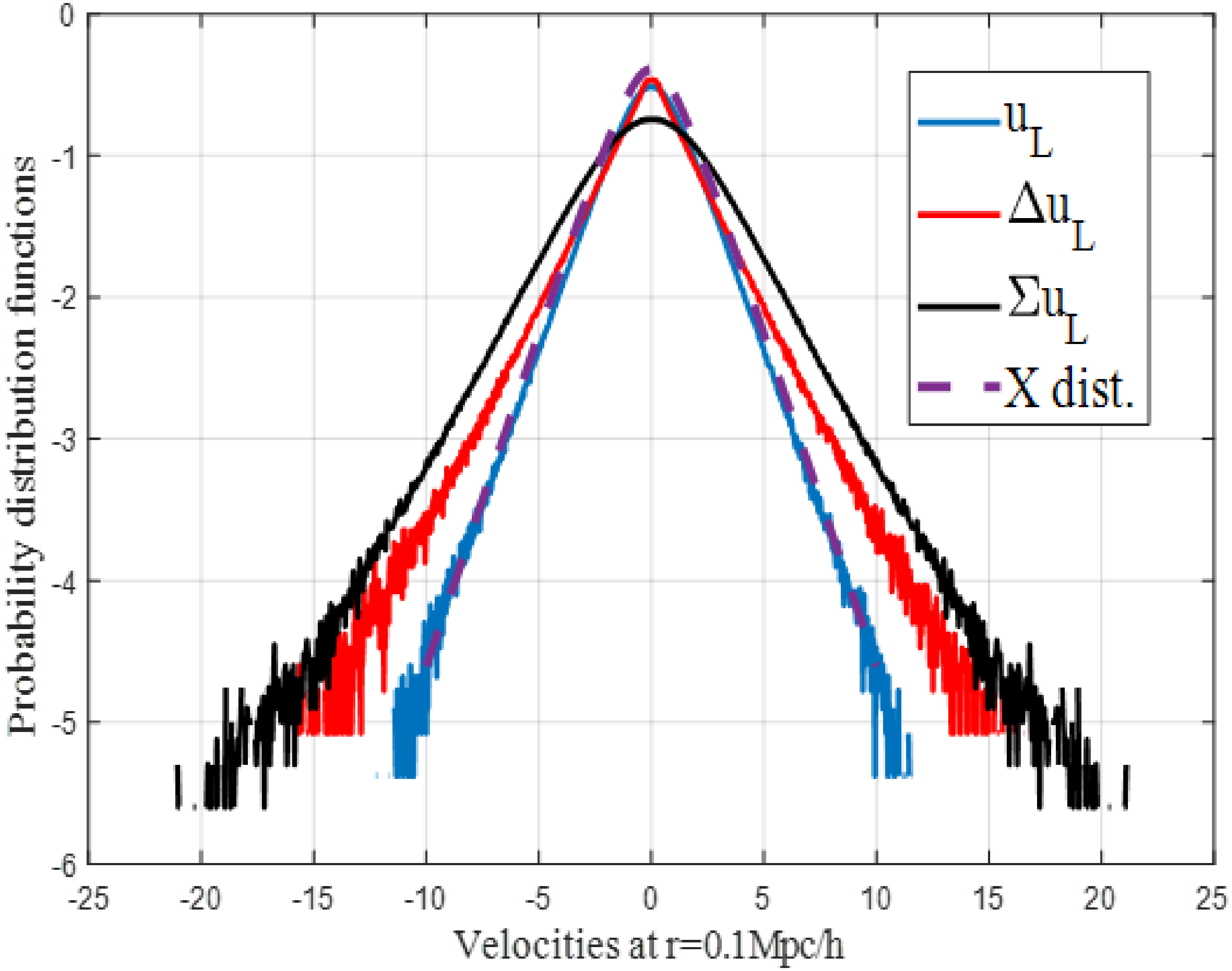

Distributions of velocities on scale of r=0.1Mpc/h at z=0

Distribution of pairwise velocity on small scale

Pacific Northwest NATIONAL LABORATORY

- On small scale, velocities u_L and Σu_L follows X distribution.
- Distribution of pairwise velocity Δu_L is different with moment estimated.
- Pairs of particles with same r can be from halos of different size.

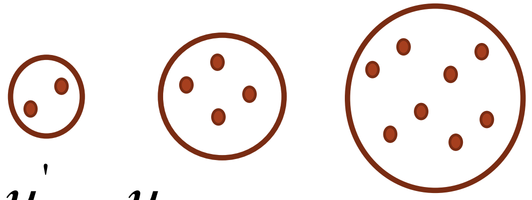

$$\Delta u_L = u_L^{'} - u_L$$

Key: correlation between two longitudinal velocities decreases with halo size:

$$\rho_{cor}\left(m_h\right) = \sigma_h^2 / \sigma^2$$

Double-λ halo mass function:

$$f\left(\nu\right) = f_{D\lambda}\left(\nu\right) = \frac{\left(2\sqrt{\eta_0}\right)^{-q}}{\Gamma\left(q/2\right)} \nu^{q/2-1} \exp\left(-\frac{\nu}{4\eta_0}\right)$$

$$P_{\Delta uL}\left(x\right) = \int_0^\infty \frac{1}{\sqrt{2\pi}\sqrt{2\left(1-\rho_{cor}\right)}\sigma} e^{-x^2/\left[4\left(1-\rho_{cor}\right)\sigma^2\right]} \beta_p f\left(\nu\right) \nu^p d\nu$$

The limiting distributions of velocity fields on small and large scales

	Velocity fields	Distribution	4th Kurtosis	6th Kurtosis	8th Kurtosis
$r \to 0$	$u_L, \Sigma u_L$	N-body, z=0, Fig. 14	**4.8**	**57**	**1200**
$r \to 0$	Δu_L	N-body, z=0, Fig. 14	7.5	160	6000
$r \to 0$	$u_L, \Sigma u_L$	$X(x)$	4.6	48.9	944.8
$r \to 0$	Δu_L	Eq. (80)	7.7	159.24	6356
$r \to \infty$	$\Delta u_L, \Sigma u_L$	N-body, z=0, Fig. 14	**4.181**	**41.46**	**670.8**
$r \to \infty$	u_L	N-body, z=0 Fig. 14	5.39	85.78	2800
$r \to \infty$	$\Delta u_L, \Sigma u_L$	Logistic (Eq. (82))	4.2	279/7	685.8
$r \to \infty$	u_L	$P_{uL}(x)$(Eq. (85))	5.4	78.4	2269.8
Exponential??		Laplace distribution	6	90	2520
		Gaussian distribution	**3**	**15**	**105**

Generalized kurtosis:

$$K_{2n}\left(\Delta u_L\right) = \frac{(2n)!}{n!2^n} \frac{\Gamma\left(n+p+q/2\right)\left[\Gamma\left(p+q/2\right)\right]^{n-1}}{\left[\Gamma\left(1+p+q/2\right)\right]^n}$$

Velocity distributions on intermediate scale

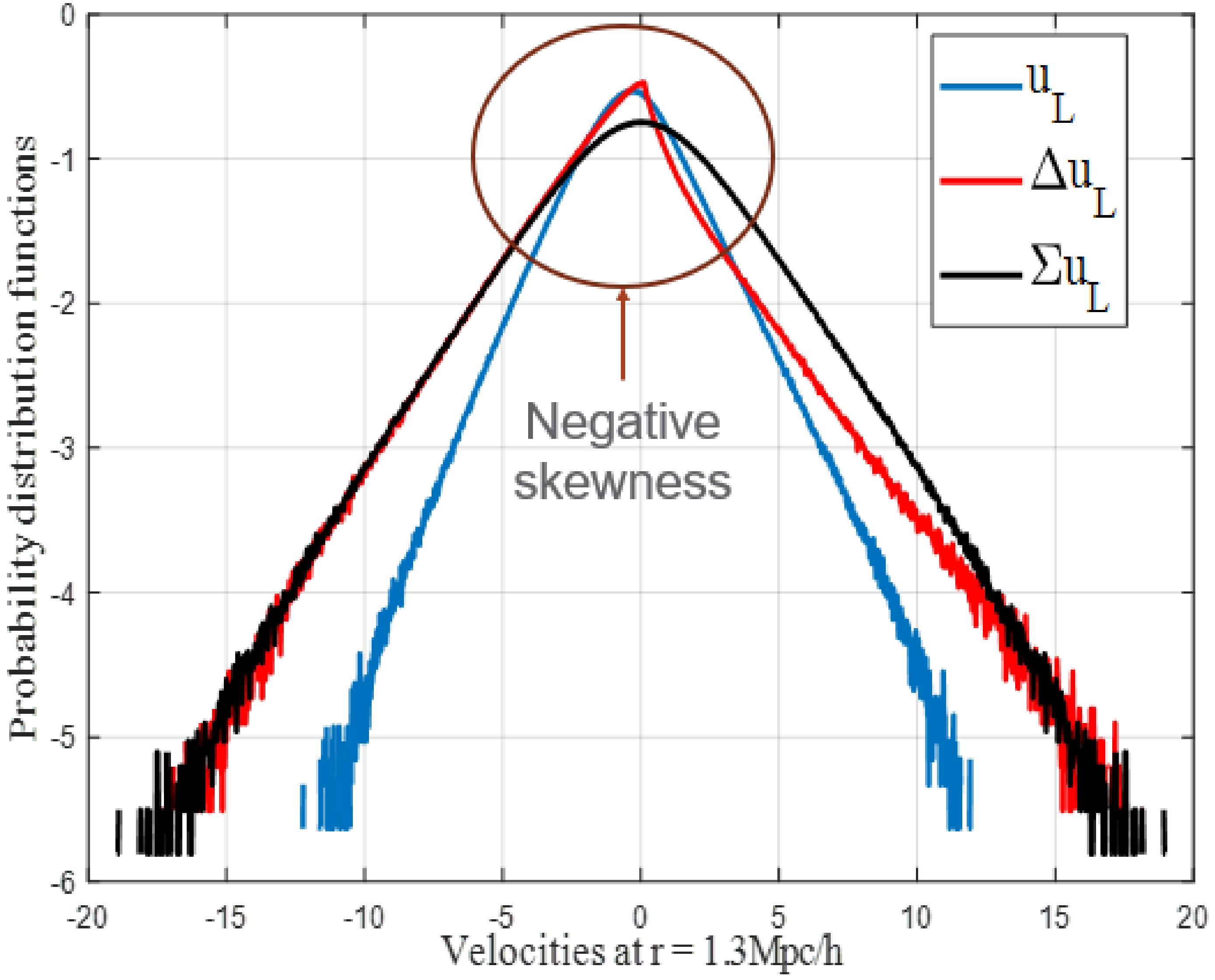

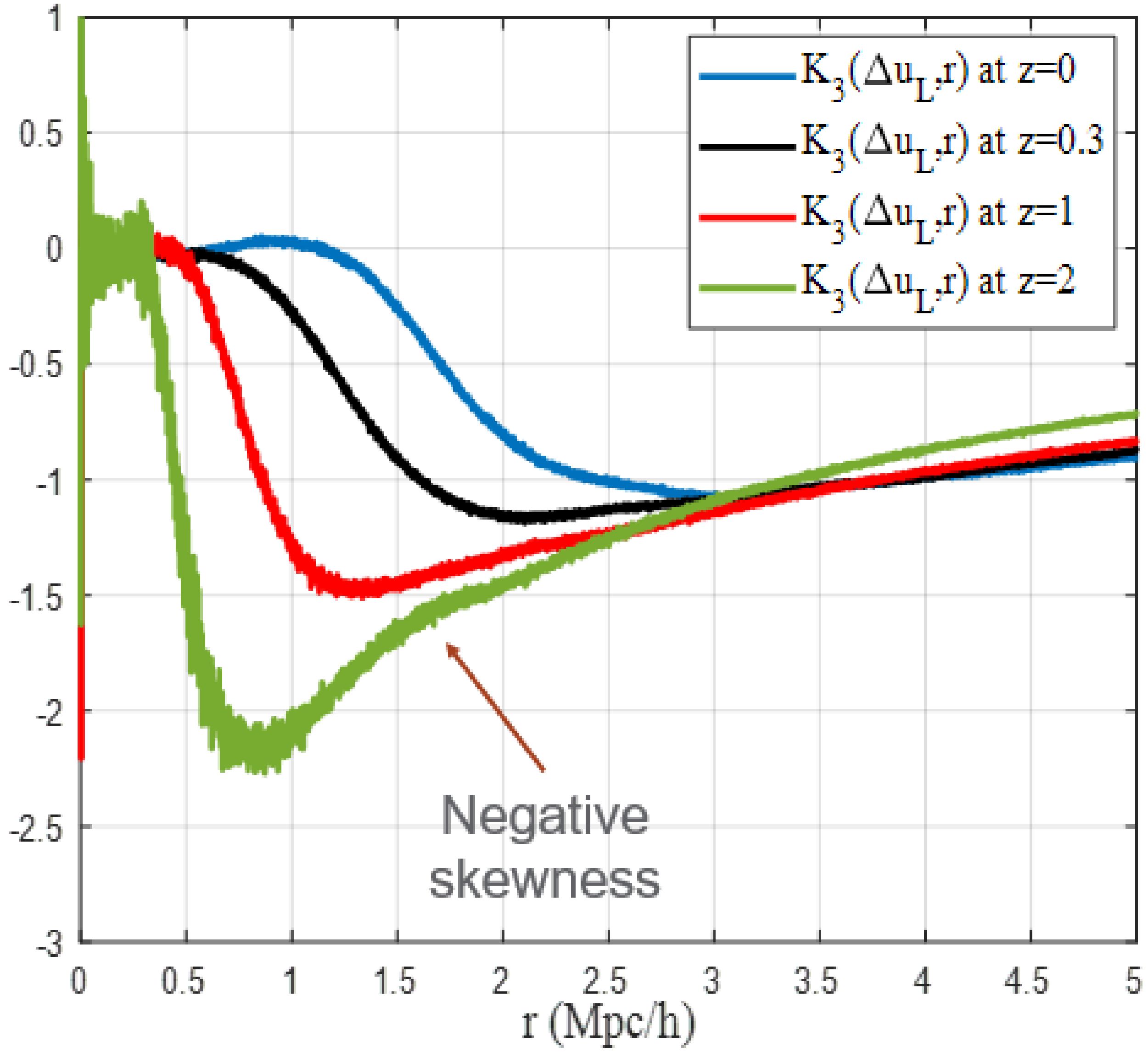

Distribution of Σu_L is symmetric, while the distribution of Δu_L is non-symmetric with non-zero (negative) skewness and skew toward positive side. This is a necessary feature of inverse energy cascade.

Modeling velocity distributions on large scale

- Distribution of Δu_L on large scale is usually assumed to be exponential in literature (non-smooth).
- This seems not agree with N-body simulation
- On large scale, Both Σu_L and Δu_L can be modelled by a logistic distribution.

Logistic distribution for both velocities:

$$P_{\Delta u_L}(x) = \frac{1}{4s}\operatorname{sech}^2\left(\frac{x}{2s}\right)$$

Reduce to exponential at large velocity:

$$P_{\Delta u_L}(x \to \infty) \approx \frac{1}{s}\exp\left(-\frac{x}{s}\right)$$

Longitudinal velocity u_L should satisfy for $\rho_L=0$:

$$P_{\Delta u_L}(z) = \int_{-\infty}^{\infty} P_{u_L}(x) P_{u_L}(z-x)\,dx$$

$$MGF_{P_{u_L}}(t) = \sqrt{\frac{\pi s t}{\sin(\pi s t)}}$$

Moment generating function for u_L

Exponential distribution

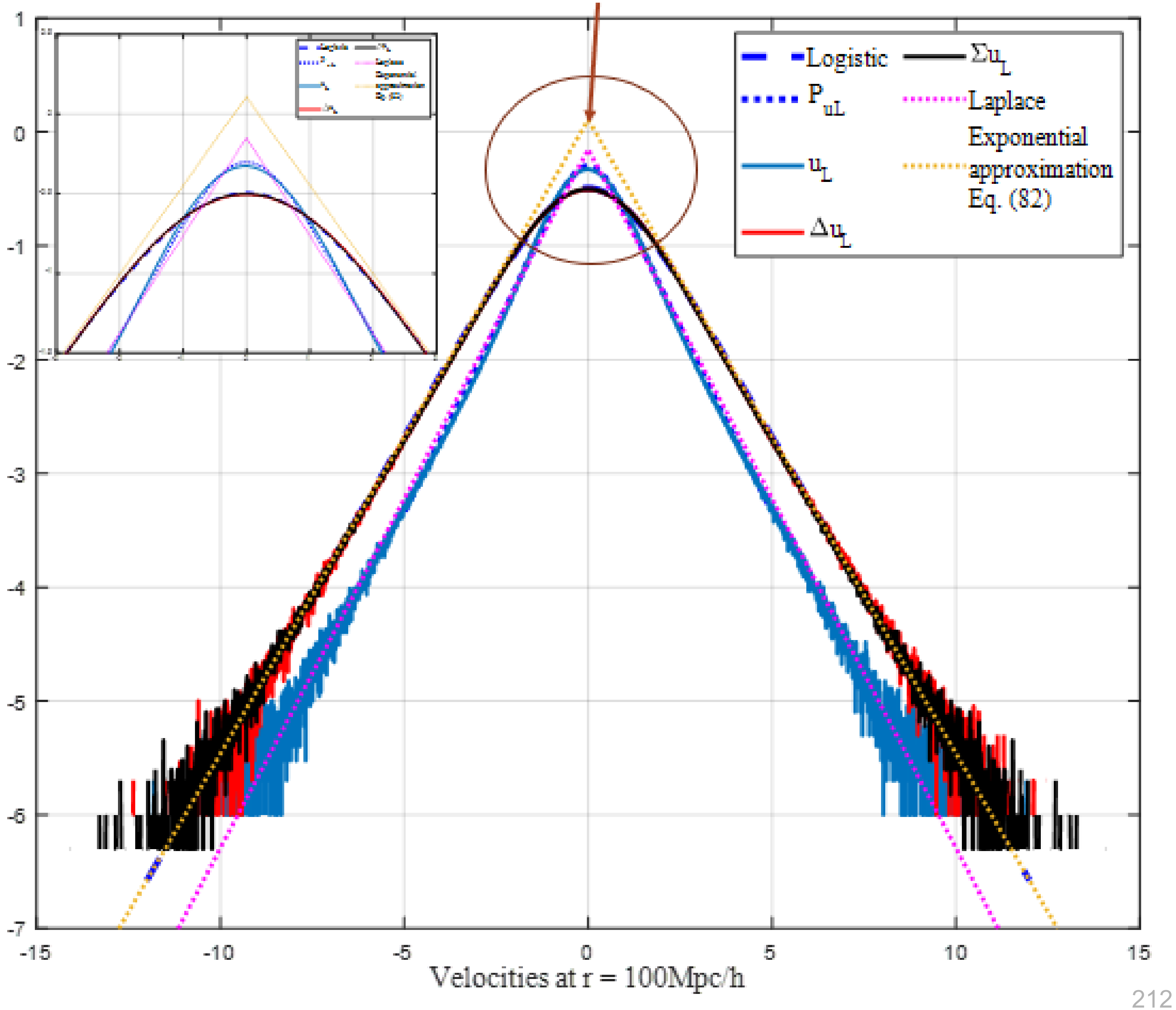

The redshift evolution of velocity distributions

- Distribution of different types of velocities changes due to redshift evolution of α.
- Shape parameter α decreases with time.
- Most velocities follows the X distribution to maximize system entropy
- Halo velocity and out-of-halo particle velocity evolves much slower than halo particle velocity due to weaker gravity on large scale.

Generalized kurtosis of X distribution:

$$K_m(X) = \left(\frac{2K_1(\alpha)}{K_2(\alpha)}\right)^{m/2} \frac{\Gamma((1+m)/2)}{\sqrt{\pi}} \cdot \frac{K_{(1+m/2)}(\alpha)}{K_1(\alpha)}$$

Plot K4 vs. K6, K4 vs. K8, and K4 vs. K10;

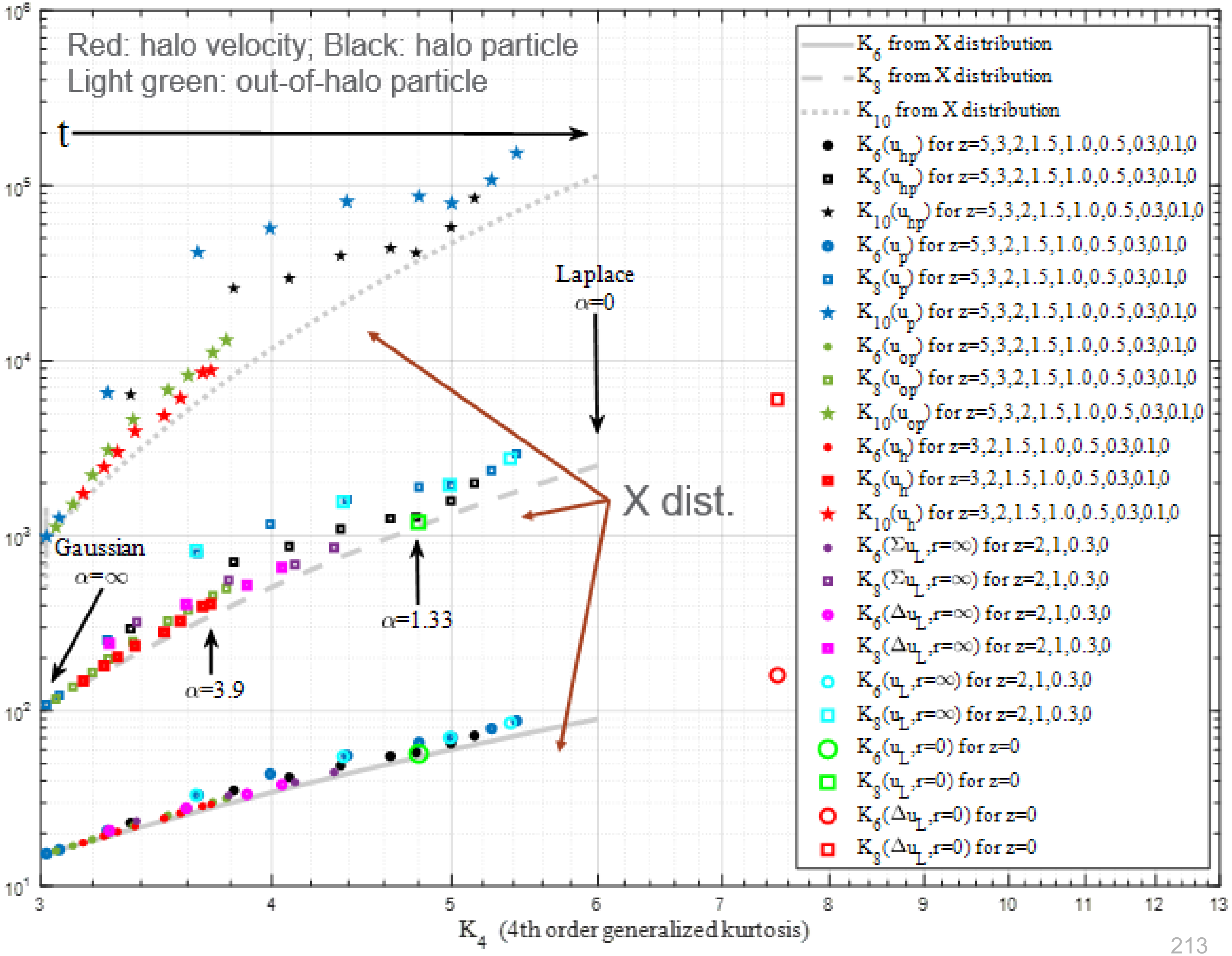

Summary and keywords

Delaunay tessellation	Pairwise velocity	Skewness
Generalized kurtosis	Velocity sum	Generalized stable clustering
Two-thirds law	X distribution	Pair conservation equation

- A halo-based non-projection approach is proposed to study the scale and redshift dependence of density and velocity distributions in dark matter flow.
- A two-thirds law for pairwise velocity was established, i.e. S_2^{lp}-$2u^2 \sim \varepsilon_u r^{2/3}$, where r is the separation between pair of particles and ε_u is the constant rate of energy cascade.
- Two-thirds law can be generalized to all even moments of pairwise velocity, while odd moments ~r
- The distributions of longitudinal velocity u_L, pairwise velocity Δu_L, and velocity sum Σu_L, are analytically modeled on both small and large scales
- Fully developed velocity fields are never Gaussian on any scale despite that they can be initially Gaussian.
- Delaunay tessellation is used to reconstruct the density field from N-body simulation, which results in an asymmetric density distribution with a long tail.
- Density correlation is obtained by directly counting all pairs on a given scale r along with simple analytical models for all second order density statistics.